Cosmological Phase Transition and Inhomogeneous Primordial Nucleosynthesis

Thesis Presented

by

Manabu Orito

to

the Department

of

Astronomical Science

for

the Degree of Doctor of Science

Department of Astronomical Science

School of Astronomical and Physical Science

The Graduate University for Advanced Studies

2-21-1, Osawa, Mitaka, Tokyo 181, Japan

Contents

Acknowledgment

I would like to express my sincere gratitude to Professor T. Kajino in National Astronomical Observatory Japan for many helps, comments and discussions and for the guidance of my thesis. I have enjoyed fruitful collaborations with him through the entire course of my graduate study.

I also would like to acknowledge Professor S. Miyama, Professor R. Ogasawara in National Astronomical Observatory for the continuous encouragements during my graduate study.

I also thank Professor G. J. Mathews in Notre Dame University and Professor R. N. Boyd in Ohio State University for their kind helps and valuable discussions. Thanks are also due to Professor G. M. Fuller in University of California and Professor C. J. Hogan in University of Washington for their valuable suggestions and discussions.

I also wish to thank Professor H. Suganuma in Osaka University for helpful discussions and suggestions on the way of calculations of nucleation rate.

I would like to acknowledge Dr. J. Kersten in University California, N. Terasawa in RIKEN and Dr. A. Hecker in Fermi Laboratory for discussions and suggestions on the evolution of inhomogeneities.

It is my great pleasure to thank Professor S. Hirenzaki, Dr. T. Kamio, K. Sumiyoshi in RIEKN, M. Mizoguchi, T. Watabe in Ruhr-University Bochum, Y. Yamamoto, Y. Sugahara in RIKEN, K. Suzuki, K. Kajihara, T. Shigetani in RIKEN, H. Monden , H. Yamamoto and S. Sasaki for their kind helps, encouragements, fruitful discussions, and valuable advises through the course of my graduate study.

I wish to thank Prof. H. Toki in RCNP and K.-I. Kubo in Tokyo Metropolitan University for providing me with the chance of graduate study and for their kind helps, encouragements through the course of my graduate study.

Finally, I would like to express my acknowledgments to all the members of the Theoretical Astrophysics Group of National Astronomical Observatory for their helps and many valuable discussions.

Abstract

We study the quark-hadron phase transition in the early Universe and the effect of baryon density inhomogeneities that emerge from this transition on primordial nucleosynthesis. We try to make clear the relation between the QCD parameters and the astronomical observable and to find the observational constraints on these parameters. We calculate the amplitude of baryon-number fluctuations and the mean separation distance between fluctuations using the finite temperature effective theory. We then analyze primordial nucleosynthesis in an environment with these inhomogeneous distribution of baryon density and compare the predicted elemental abundance with observation. Through the comparison of these calculation with the observation, we discuss the sensitivity of elemental abundance to the physical condition of baryon density inhomogeneities.

We first estimate the nucleation rate of hadron bubble during the supercooling epoch and study the evolution of baryon-number density at the constant-temperature coexistence epoch. We calculate the baryon permeability through the phase boundary using the chromoelectric flux tube model. In this calculation, we consider the temperature dependence of the constituent quark mass and that of the string tension suggested from lattice QCD simulation. We find that although the flux of baryons evaporating from QGP is strongly depend on the quark mass and string tension at critical temperature, this flux is still sufficiently small, suggesting that the baryon number is no easily transferred from QGP to hadron phase. For realistic value of quark mass and string tension The resultant amplitude of baryon density fluctuation is very huge and have a significant effect on primordial nucleosynthesis yields.

We then study the inhomogeneous primordial nucleosynthesis in order to compare with observational constraints. we consider the effects of fluctuation geometry on primordial nucleosynthesis. For the first time we consider condensed cylinder and cylindrical-shell fluctuation geometries in addition to condensed spheres and spherical shells. We also consider implications of the possible detection of a high D/H abundance in a Lyman-*alpha* absorption cloud at high redshift and implied chemical evolution effects of a high deuterium abundance. We find that a cylindrical shell geometry allows for an appreciably higher baryonic contribution to be the closure density ($\Omega_b \leq 0.2$) than that allowed in spherical inhomogeneous or standard homogeneous big bang model. We

also find that inhomogeneous primordial nucleosynthesis in the cylindrical shell geometry can lead to significant Be and B production. $[\mathrm{Be}] = 12 + \log(\mathrm{Be/H}) \approx -3$ is possible while still satisfying all of the usually adopted light-element abundance constraints.

§1 Introduction

The Hubble expansion of galaxies, the 2.73 K black body radiation background argue for a hot, dense origin of the universe, the hot big-bang cosmology. As a consequence, the early Universe could be a primordial nuclear reactor in which the light nuclides D, ^{3}He, ^{4}He, and ^{7}Li were synthesized in astrophysically interesting abundances. This nuclear reactions took place from an expansion age of 0.01 sec to 100 sec corresponding to the temperature from 10 MeV to 0.1 MeV. The comparison of the predicted abundance with observationally inferred primordial abundance provide, therefore, the earliest test of the big bang cosmology. Based on a simple set of assumptions (isotropy and homogeneity: validity of general relativity: no particle degeneracy: thermodynamic equilibrium: homogeneous baryon density distribution) the homogeneous big bang nucleosynthesis (HBBN) model is able to reproduce the observationally inferred light element abundance using only one free parameter, the baryon-to-photon ratio η. Since the abundances of these primordial isotopes span some ten orders of magnitude, this is an impressive success for big-bang cosmology. Furthermore, recent results from the LEP and SLC collider studies on the width of the Z^0 particle (Aarnio et al. 1989; Abrams et al. 1989; Adeva et al. 1992; Denegri, Sadoulet, & Spiro 1990), which are $N_\mu = 2.988 \pm 0.023$, are in excellent agreement with the complimentary constraint on the number of relativistic neutrino families, $N_\mu < 3.3$, predicted by HBBN theory [e.g., Steigman, Schramm & Gunn 1977; Olive et al. 1990; Walker et al. 1991] even before these measurements were carried out.

Big-bang nucleosynthesis further provides important information about the density of baryons in the Universe since the predicted abundance of light element depends on the baryon density of the universe. In fact, primordial nucleosynthesis provides the

most precise determination of the baryon density in the universe quantitatively from the real data of elemental abundances in old stellar objects.

Universal mass consists of luminous and dark objects. The luminous component is made of atomic nuclides in stars and galaxies which electromagnetically interact with photons and thus called luminous matter. It takes only a small mass fraction less than one percent of the critical mass $\Omega_b{}^{(LUM)}(OBS) \leq 0.01$ (Jedamzik, Mathews & Fuller 1995) , where $\Omega_b = \rho_b/\rho_c$, $\rho_c = 3H_0^2/8\pi G$ is the critical density to close the Universe marginally, and H_0 is the Hubble constant ranging $0.8 < h_{50} = H_0/50(km/s/Mpc) < 2.0$. On the other hand, dynamical mass in the largest scale of the cluster of galaxies is observed to be very large $\Omega_{DYN}(OBS) = 0.1 - 0.3$, suggesting clearly that more than 90% of the total universal mass originates from dark matter.

It is useful to classify the dark matter in several ranks (Kajino 1991a). If it consists of baryons, it is called baryonic dark matter. The primordial baryonic dark matter candidate is the strange quark matter nugget or mini black hole. Since these baryonic objects are created in the cosmological phase transition before the recombination epoch, they are almost free from gravitational dissipation and can even distribute over the galactic halo as well, making a remarkable contribution to the total Ω if they survive until today. The second rank of baryonic dark matter is the stellar black hole, neutron star, or brown dwarf. Another rank is non-baryonic dark matter. Its candidate is more or less hypothetical, including massive light neutrino, heavy neutrino, SUSY particle like gravitino, photino, Higgsino, Glueino, or non-thermal particle like axion, monopole, soliton, etc. The CERN experiment (ALEPH collaboration 1990) of measuring the decay products from neutral weak boson ruled out WIMPs of cosmological interest having a mass smaller than 45 GeV and that the generation of the light neutrino family was determined to be three. In spite of many other experimental searches, however,

there is unfortunately no definite signal of the detection of these non-baryonic dark matter candidates yet.

Quite recently, several astronomical detections (White et al. 1993; White and Fabian 1995) of hot X-rays from dense galactic clusters have indicated that more baryons than ever known may exist in the form of hot ionized gas. Their contribution to Ω is estimated to be $\Omega_b \lesssim 0.22 h_{50}^{-1.5}$ Another recent discovery (Alcock, Fuller, & Mathews 1987,Aubourg et al. 1993) of MACHOs (massive astronomical compact halo objects), which are presumed to be brown dwarfs or Jupiter size small mass stars, suggests that the dark matter in the galactic halo is most likely baryonic. Their expected (Freeman 1994) mass density is $\Omega_b \gtrsim 0.09$. These recent observations show one order of magnitude larger baryonic mass than the luminous, and is in reasonable agreement with the total dynamical mass $\Omega_{DYN}(OBS) = 0.1 - 0.3$. It is therefore a challenging and even realistic assumption that the major part of dark matter is baryonic.

The homogeneous big bang nucleosynthesis (Wagoner, Fowler, & Hoyle 1967; Wagoner 1973; Walker et al. 1991; Smith, Kawano, & Malaney 1993; Copi, Schramm & Turner 1995; Schramm & Mathews 1995), which assumes homogeneous distribution of baryons, limits the contribution from baryonic mass as small as $\Omega_b h_{50}^2 \approx 0.06$, from the light element abundance constraints. If the homogeneity assumption is a good approximation, the nature of dark matter must be non-baryonic. This conclusion is apparently inconsistent with several recent observations suggesting $0.09 \lesssim \Omega_b \lesssim 0.22$, as discussed above. In addition to that inconsistency, recent developments in measurements of primordial light element abundances, in particular deuterium and helium, has suggested a possible conflict between the predicted abundances of the light element isotopes from HBBN and the abundances inferred from observations.

In the Standard Hot Big Bang model it is assumed that the universe has expanded

from an initial state of very high temperature and density. The thermodynamic history of the universe can be discussed back to times just after the Plank time $t \sim 10^{-43}$ sec, at which point the temperature and density are $T \sim 10^{19}$ GeV and $\rho \sim 10^{78}$ GeVfm^{-3}, respectively. Although recent observations (Smoot et al. 1992; de Bernardis et al. 1994a) of the cosmic microwave background anisotropy may provide some glimpse of conditions in the universe near the Planck time when the universe was in the inflationary epoch (Davis et al. 1992; de Bernardis et al. 1994b), we still have no direct proof that the universe ever was such extreme conditions. Indeed although it only extrapolates back to times of $t \sim 10^{-2}$ sec, where $T \sim 10\,\mathrm{MeV}$ and $\rho \sim 100\mathrm{g\ cm}^{-3}$, primordial nucleosynthesis is still the best direct probe of the young universe. Careful and detailed studies of variant nucleosynthesis scenarios are, therefore, necessary not only to solve the inconsistency between the theory and observation in recent years and also to quantify the physical conditions of the early universe. Similarly, the yields from primordial nucleosynthesis are very sensitive to conditions in the early universe. Therefore, the observed primordial isotopes can probe the physics of variant cosmological models which may have been determined at times earlier than those addressed in the primordial nucleosynthesis.

There has been interest in problems at the interface of cosmology and particle physics in the past decade. The application of the standard model of high energy physics ($\mathrm{SU(3)_c} \otimes \mathrm{SU(2)} \otimes \mathrm{U(1)_Y}$) to big ban cosmology strongly suggests that as the temperature was cooled, the universe underwent several cosmological phase transitions during its early evolution. In the temperature interval between roughly 1 TeV and 100 MeV, the universe has experienced the rich physical phenomena: electroweak symmetry breaking ($t \approx 10^{-10}$sec), chiral symmetry breaking ($t \approx 10^{-4}$sec), and quark confinement/deconfinement transition, in which free quarks and gluons were confined

into hadrons in quantum chromodynamics (QCD) all occur in this interval. Although we can imagine theoretically what happened in this phase transition, there has been no observational signature until recently showing the physical processes operated at this epoch. The properties of these transition can all be constrained using primordial nucleosynthesis which occur soon after the QCD phase transition.

Cosmological QCD phase transition is of particular interest among them because much knowledge has been accumulated by a number of theoretical studies of QCD and it is matured to apply them to the physics of the phase transition. In addition, recent lattice gauge simulation (Iwasaki et al. 1995) of full QCD has suggested it is of first order, which leads to a direct impact on the creation of inhomogeneous baryon distribution as first pointed out by Witten (Witten 1984).

Witten realized that baryon number would be concentrated in the quark phase if baryon chemical equilibrium could be established, and that the transport of baryon number at the phase boundary was such that baryon number concentration could occur. This result suggests that large-amplitude baryon density inhomogeneities could be produced in the QCD phase transition. This baryon inhomogeneities produced in the QCD phase transition could give rise to a very rich set of scenarios for primordial nucleosynthesis because the effects of varying baryon-photon ratio and the diffusion of neutrons into low-baryon density region which cause a variation of the neutron-to-proton ratio (Applegate, Hogan & Scherrer 1987).

There are other mechanism of creating baryon inhomogeneity in some cosmological phase transition before an onset of primordial nucleosynthesis has been wanted. There are a lot of mechanisms proposed for that, such as inflation generated isocurvature fluctuations (at GUTS era, $t \approx 10^{-34}$sec), baryogenesis associated with a first order electroweak phase transition at EW era, kaon condensation after the QCD epoch, mag-

netic fields driven by a motion of superconducting cosmic strings (after $t \approx 10^{-34}$sec), and so on.

The first purpose of this thesis is to discuss the creation mechanism of baryon inhomogeneity in the first order QCD phase transition and try to make clear the physical condition on the fluctuation amplitude, length scale and others, in terms of the QCD parameters. The second purpose is to discuss the impact of the QCD physics on several cosmological problems.

It is a common misconception that the most natural amplitude for baryon-number fluctuations is just that given by the thermodynamic ratio of equilibrium baryon densities in the two phases of a QCD phase transition. This is as a number ~ 100 for the QCD phase transition (Witten 1984; Alcock, Fuller, & Mathews 1987). This value for the fluctuation amplitude, however, is unlikely. It would occur only if complete equilibrium were maintained in both phases until near the end of the phase transition followed by a sudden complete drop from equilibrium. This would require efficient mixing of baryon number across the phase boundary until just near the end of phase transition. However, the property of baryon number transport from the quark-gluon plasma to the hadron phase is governed by strong interaction described by QCD since there are no baryon number violating processes occurring during the QCD phase transition and baryon number has to physically transport across the moving phase boundary as nucleated bubbles of hadron phase grow. This process corresponds to three color-singlet quarks moving toward and through the phase boundary to produce baryon. We estimate this transport in the context of the chromoelectric flux tube model (Sumiyoshi et al. 1989; Sumiyoshi, Kajino, Alcock & Mathews 1990; Kajino et al. 1996) which has been used to describe baryon production in hadron showers on high energy collider experiment. In this picture the baryon number transport occurs when a flux tube appears

outside the phase boundary. We also include the effect of the temperature dependence of quark mass and string tension in flux tube (Kajino et al. 1996). The formation of baryons is significantly hindered with realistic quark mass and string tension which can lead to the production of large baryon number density fluctuations in the regions of shrinking quark-gluon plasma. Therefore, baryon inhomogeneities induced by QCD phase transition can affect primordial nucleosynthesis yields. We adopt typical value of fluctuation amplitude given by the calculation mentioned above when we explore the effect of inhomogeneities on primordial nucleosynthesis.

We show that inhomogeneous big-bang model for primordial nucleosynthesis (Applegate, Hogan & Scherrer 1987; Kajantie & Kurki-Suonio 1986; Alcock et al. 1993; Malaney & Fowler 1988; Mathews, Kajino & Orito 1996) (hereafter IBBN) allows higher universal mass density parameter $\Omega_b \lesssim 0.2$ which is a very charming result Mathews, Kajino & Orito 1996 providing a possible solution to the dark matter problem only by baryons. In this model the initial distribution of nuclear fuels, protons and neutrons, is taken to be largely inhomogeneous as a consequence of first order cosmological phase transition which proceeds in an inhomogeneous manner of space-time evolution. Such a characteristic circumstance makes a dramatic effect on the primordial nucleosynthesis on heavy elements (Boyd & Kajino 1989; Kajino & Boyd 1990; Kajino, Mathews & Fuller 1990; Jedamzik, Fuller & Mathews 1994) , still satisfying the light element abundance constraints for D, ^{3}He, ^{4}He and ^{7}Li.

In the previous studies of IBBN model it has been generally assumed that the fluctuation geometry of baryon density distribution is spherical. However, this geometry require sufficient surface tension to localize shrinking quark-gluon plasma. Several recent lattice QCD calculations indicate that the surface tension is too small to allow spherical fluctuation geometry. And also, recent simulation of QCD phase transition

(Freese & Adams 1990) indicate that the structure of fluctuation can be cylindrical geometry. The physical motivated geometry, therefore is uncertain.

The second purpose of this thesis is, therefore, to explore the sensitivity of the predicted elemental abundances in IBBN models to the geometry of the fluctuations. We consider here various structures and profiles for the fluctuations in addition to condensed spheres. Mathews et al. (1990, 1994, 1996) found that placing the fluctuations in spherical shells rather than condensed spheres allowed for lower calculated abundances of ^{4}He and ^{7}Li for the same Ω_b, and that a condensed spherical geometry is not necessarily the optimum. Here we show that a cylindrical geometry also allows for an even higher baryonic contribution to the closure density than that allowed by the usually adopted condensed sphere. It appears to be a general result that shell geometries allow for a slightly higher baryon density. This we attribute to the fact that, for optimum parameters, shell geometries involve a larger surface area to volume ratio and hence more efficient neutron diffusion.

An important possible consequence of baryon inhomogeneities at the time of nucleosynthesis may be the existence of unique nucleosynthetic signatures. Among the possible observable signatures of baryon inhomogeneities already pointed out in previous works are the high abundances of heavier elements such as beryllium and boron (Boyd & Kajino 1989; Kajino & Boyd 1990; Malaney & Fowler 1989; Terasawa & Sato 1990; Kawano et al. 1991), intermediate mass elements (Kajino, Mathews & Fuller 1990), or heavy elements (Malaney & Fowler 1988; Applegate, Hogan & Scherrer 1988; Rauscher et al. 1994).

The nuclear reaction flow stops at $A = 7$ in HBBN because of the instability of ^{8}Be. In the IBBN, however, where the nucleosynthesis occurs in an environment of proton/neutron inhomogeneous distribution, the radioactive nuclear reactions become

active in order to create intermediate-to-heavy mass elements via the production of unstable nuclei ^{8}Li(838 ms),^{9}Li(178.3 ms),^{7}Be(53.29 d), ^{10}Be(1.6$\times$106 y), $\underline{8}$(770 ms) etc. Such possible signatures are also constrained, however, by the light-element abundances. It was found in several previous calculations that the possible abundances of synthesized heavier nuclei was quite small (e.g., Alcock et al. 1990; Terasawa & Sato 1990; Rauscher et al. 1994). We find, however, that substantial production of heavier elements may nevertheless be possible in IBBN models with cylindrical geometry.

§2 Cosmological QCD Phase transition

A first order QCD phase transition (Iwasaki et al. 1995) is a viable cosmological site for the creation of baryon inhomogeneity (Witten 1984). When the expanding Universe first cooled to the critical temperature $T_c \approx$150MeV at $t_c \approx 10^{-4}$ sec, hadron bubbles are nucleated in the sea of quark gluon plasma (QGP) at the supercooling epoch. Liberated latent heat continuously reheats the Universe to sustain $T = T_c$ again after the nucleation stops. Two phases, QGP and hadron gas, can coexist now and hadronic bubbles grow gradually towards the end of the phase transition. The baryon number which was originally carried by only net quarks inside QGP is transported to the hadron gas phase through the phase boundary.

The dynamics of the QCD phase transition is phenomenologically described in terms of four fundamental parameters in QCD (Fuller, Mathews, & Alcock 1988). They are the critical temperature of the phase transition, T_c, the intrinsic surface tension of the phase boundary between the high-energy QGP phase and low-energy hadron gas phase, σ, the latent heat of the phase transition, L, and the baryon permeability through the phase boundary λ. Only the order of these parameter values, except for the last one λ, are incompletely known from lattice gauge QCD, i.e. $T_c \approx$ 100MeV (in full QCD) and 200 MeV, $L \approx T_c^4$, and $\sigma \approx 0.01 T_c^3$. We therefore take T_c and σ as free parameters in a reasonable suggested range, i.e. 70MeV$\leq T_c \leq$ 200MeV and $\sigma \leq 10^7$MeV^3 , and let L obey the free gas approximation. Namely, the condition of pressure equilibrium between the free quarks and gluons in QGP phase and the free pions in hadron gas phase leads to $L = 4(g_q - g_h)T_c^4$, where the statistical weight for each phase is given by $g_q = g_Q + g_{\gamma l}$, $g_h = g_H + g_{\gamma l}$, $g_Q = 37$, $g_H = 3$ and $g_{\gamma l} = 14.25$ (Bessell & Norris 1984) is the background contribution from photons (γ) and leptons ($l = n_{e,\mu,\tau}, e^-, \mu^-$

and their anti-particles). It is challenging to calculate these fundamental parameters precisely in QCD theory.

A necessary ingredient for any quantitative discussion of the phase transition is an explicit form for the equation of state. We first consider the thermodynamics of the quark-hadron phase transition.

2-1 Thermodynamical Aspects of QCD Phase Transition

It will be most convenient for our purpose to compute the thermodynamic potential Ω for both the quark-gluon plasma phase and the hadron phase. We caution that we have used the symbol Ω for both the thermodynamic potential and the density parameter for the universe. It should be clear from the context which we intend.

The thermodynamic variable corresponding to Ω are

$$P = -\left[\frac{\partial\Omega}{\partial V}\right]_{T,\mu} = -\Omega/V, \tag{II-1}$$

$$n = -\frac{1}{V}\left[\frac{\partial\Omega}{\partial\mu}\right]_{V,T}, \tag{II-2}$$

$$S = -\left[\frac{\partial\Omega}{\partial T}\right]_{V,\mu}, \tag{II-3}$$

$$E = -PV + ST + \mu nV, \tag{II-4}$$

where P, n, S, and E are respectively, the pressure, particle number density, entropy, and energy.

A first-order phase change occurs when there are two physically distinct organizations of the statistical degree of freedom which can occur for the same T, μ. The more stable phase has the lower Ω (higher P), and the two phases coexist when $P_q = P_h$ (where q = quark phase, h = hadron phase), which yields a coexistence curve $T = T_c(\mu)$.

In the early Universe, because of the baryon-to-entropy ratio is very small (unless the enrichment is extreme), we shall limit ourselves to the case $\mu << T$.

The latent heat per unit volume in the phase change is

$$L = T_c \frac{\partial}{\partial T}(P_q - P_h) = T_c(s_q - s_h), \tag{II-5}$$

where the derivative is evaluated at constant μ and at $T = T_c$, and s_q and s_h are entropy densities in the quark-gluon and hadron phase, respectively.

It is straightforward to compute the grand partition function, and thus Ω, if we assume that the particles are noninteracting except for an overall QCD vacuum energy in the unconfined phase. The background relativistic particles which are no strongly interacting and are in thermal equilibrium with both the confined and unconfined phases contribute

$$\Omega = -V(g_b + \frac{7}{8}g_f)\frac{\pi^2}{90}T^4, \tag{II-6}$$

where g_b and g_f are the statistical weights of bosons and fermions, respectively. At the epoch of the quark-hadron phase transition photon, electrons, muons, and neutrinos yield $g = g_b + \frac{7}{8}g_f = 14.25$.

We treat the unconfined quark-gluon plasma as a gas of noninteracting relativistic particles plus an overall vacuum energy. In the limit of vanishing quark masses, there is a simple expression for Ω which is valid for any temperature and chemical potential

$$\begin{aligned} \Omega_{qg} &= \frac{-7\pi^2}{180}N_c N_f V T^4 \left[1 + \frac{30}{7\pi^2}\left\{\frac{\mu_q}{T}\right\}^2 + \frac{15}{7\pi^4}\left\{\frac{\mu_q}{T}\right\}^4\right] \\ &- \frac{\pi^2}{45}N_g V T^4 + BV. \end{aligned} \tag{II-7}$$

Here N_c is the number of colors (3), N_f is the number of relativistic quark flavors (2 at lower temperatures corresponding to the u and d quarks, and 3 at higher temperatures where the strange quark becomes relativistic), and B is the QCD vacuum energy, or bag

constant. The number of gluons is $N_g = 8$. The quark chemical potential is $\mu_q = \mu_b/3$, where μ_b is the baryon chemical potential.

The QCD vacuum energy contributes negatively to the pressure. The value of this vacuum energy, or bag constant, is not known and in what we have done it serves to parameterize the temperature at which the confined and unconfined phases coexist. the numerical examples suggest that the value of bag constant is $B = 780\,\mathrm{MeV/fm^3}$.

For the confined, or hadronic, phase we take the fluid to consist of an ideal gas of massless pions and of massive nucleons with Maxwell-Boltzmann statistics. Then

$$\Omega_h = -\frac{g_h \pi^2}{90} T^4 + \left[\frac{2mT}{\pi}\right]^{3/2} \cosh(\mu/T)\exp(-m/T), \tag{II-8}$$

where g_h is total statistical weight in the hadron phase. At $T = T_c \approx 100\,\mathrm{MeV}$ the value of g_h is 17.25. The total statistical weight for quark-gluon phase in coexistence is $g_q \approx 51.25$.

From the Eqs. II-6-II-8 the pressure P_q, energy density E_q, and entropy density s_q, in the quark-gluon phase are given as

$$P_q = \frac{1}{3} g_q a T^4 - B, \tag{II-9}$$

$$E_q = g_q a T^4 + B, \tag{II-10}$$

$$s_q = \frac{4}{3} g_q T^3, \tag{II-11}$$

$$\tag{II-12}$$

where $a = \pi^2/30$. For the hadron phase the corresponding quantities are

$$P_h = \frac{1}{3} g_h a T^4, \tag{II-13}$$

$$E_h = g_h a T^4, \tag{II-14}$$

$$s_h = \frac{4}{3} g_h a T^3. \tag{II-15}$$

$$\tag{II-16}$$

We define the ratio of statistical weights in the two phases to be

$$x = \frac{g_q}{g_h} = \frac{s_q}{s_h} \approx 2.971 \text{ at } \quad T_c \approx 100\,\text{MeV}. \tag{II-17}$$

Within the temperature range between 40 MeV and 240 MeV which is indicated recent studies of QCD phase transition, x is slowly varying function of temperature ($\sim 2.97 \pm 1$).

Pressure equilibrium, or coexistence, between the two phases $P_h = P_q$, occurs for a temperature

$$T_c = (g_q - g_h)^{-1/4} \left[\frac{3}{a}\right]^{1/4} B^{1/4}. \tag{II-18}$$

2-2 Nucleation of Hadron Bubbles in Supercooling Epoch

The nucleation rate is determined by probability that a spontaneous fluctuation in the metastable (quark) phase will produce a critical nucleus of the stable (hadron) phase. This critical nucleus has radius r_c determined by

$$P_h - P_q = \frac{2\sigma}{r_c}, \tag{II-19}$$

where σ is the free energy per unit surface area associated with the boundary of the nucleus, surface tension.

New nuclei with radii less than r_c will collapse and disappear, while nuclei of radii larger than r_c will expand until a macroscopic amount of new phase is produced. The probability of a fluctuation of radius r_c is $\exp(-W/T)$ where

$$W = \frac{4\pi}{3} r_c^3 (P_q - P_h) + 4\pi r_c^2. \tag{II-20}$$

The first term in II-20 is the difference between the thermodynamic potentials of the two phases and is negative. The second term is the surface free energy of the boundary between the phases.

From the Eq. (II-5) we define

$$P_h - P_q = L\eta, \tag{II-21}$$

$$\eta \equiv \frac{T_c - T}{T_c}, \tag{II-22}$$

where L is the latent heat per unit volume of the phase transition and η is the supercooling parameter. In the classical isothermal fluctuation theory (Landau & Lifshits 1969), the nucleation rate of hadronic bubbles which have a macroscopic $size \approx \mu m$ is given by

$$\Gamma_{NUC}(T) \approx T^4\{8/3 \cdot \sigma^3/T_c L^2\eta^2\}^{3/2}\exp[-16\pi/3 \cdot \sigma^3/T_c L^2\eta^2]. \tag{II-23}$$

The universal temperature as a function of time is known from Einstein equation

$$tT^2 = t_c T_c^2, \tag{II-24}$$

and the volume fraction of the supercooling phase in the horizon, f_{SC}, which is unaffected by the shock front carrying the latent heat, is statistically given (Kajantie & Kurki-Suonio 1986) by

$$f_{SC}(t) = \exp[-\int f_{SC}(t') \cdot \Gamma_{NUC}(T') \cdot 4\pi/3 V_s{}^3 (T/T')^3 (t - t')^3 dt'], \tag{II-25}$$

where V_s is the sound velocity of relativistic plasma which is representative for the velocity of the shock front. We can calculate the number density of nucleation sites, N_{NUC}, by integrating $f_{SC} \cdot \Gamma_{NUC}$ over the supercooling epoch, and obtain the mean

separation distance $\langle l_H \rangle$ between the hadronic bubbles, too.

$$N_{NUC} = \int f_{SC}(t') \cdot \Gamma_{NUC}(T') \left[\frac{R(t')}{R(t)}\right]^3 dt', \quad \text{(II-26)}$$

$$\langle l_H \rangle = {N_{NUC}}^{-1/3}. \quad \text{(II-27)}$$

These are basic quantities in order to describe the evolution of space-time structure of the mixed phase of QGP and hadron gas during the phase transition.

From Eq. (II-20) - (II-25), We can evaluate the time t_f or T_f when the entire universe has been reheated and η_f of

$$\eta_f \approx 1.4 \frac{\sigma^{3/2}}{T_c^{1/2} L} = 0.0101, \text{at } T_c = 150\,\text{MeV},\ L = 7 \times 10^9,\ \sigma = 0.1\,T_c^3. \quad \text{(II-28)}$$

The duration of nucleation epoch is short compared to the Hubble time since the fractional supercooling is small.

2-3 Dynamics of the Universe During the Constant-Temperature Coexistence Epoch

Because the duration of nucleation epoch is short, the entropy generation associated with reheating to T_c is expected to be small compared to the initial entropy. At the end of this nucleation epoch the universe is left with bubbles of hadron phase surrounded by quark-gluon plasma, all in pressure equilibrium at T_c.

In order to study the evolution of the mixed phase of QGP and hadron gas in the reheated Universe at $T = T_C$ after the nucleation ends, one has to solve the manner of expanding Universe and the volume change of the QGP phase. At the epoch of

cosmological QCD phase transition, the energy density of the background photons and leptons is very huge, $\rho_{\gamma l} = g_{\gamma l} \cdot aT^4 \approx 10^{10}(\mathrm{MeV}^4)$, $a = \pi^2/30$. Baryons have a smaller average matter density, $\rho_B \leq 10^2(\mathrm{MeV}^4)$ in the $\Omega_B \leq 1$ Universe models. Although we are interested in the inhomogeneous baryon density distribution to be formed at this epoch, it is a reasonable assumption that the Universe is globally homogeneous and isotropic if the fluctuation amplitude satisfies a condition $\delta\rho_B/\rho_B << 10^8$. Such fluctuations are still very strong, compared with the average ρ_B. The Einstein equation in Robertson-Walker metric is thus given by

$$(dR/dt)^2/R^2 = 8\pi G/3 \cdot [\rho_q f_V + \rho_h(1 - f_V)], \tag{II-29}$$

$$p \cdot dR^3/dt = d[R^3\{\rho_q f_V + \rho_h(1 - f_V)\} + R^3 p]/dt, \tag{II-30}$$

where R is the scale factor, ρ_q,ρ_h, and $p = p_q = p_h$ are the energy density and the pressure of QGP (q) and hadron gas (h) phases, and $f_V(t)$ is the volume fraction of QGP. These coupled equations are to be solved with the boundary conditions $f_V = 1(T_C \leq T)$ and $f_V = 0(T_C \geq T)$.

Equations (II-29) and (II-30 can be solved to yield

$$\frac{R(t)}{R_i} = (4x)^{1/3}\left[\cos\left\{\frac{3\chi(t - t_i)}{2(x-1)^{1/2}} + \arccos\frac{1}{2x^{1/2}}\right\}\right]^{2/3}, \tag{II-31}$$

where

$$\chi = \left[\frac{8\pi GB}{3}\right]^{1/2}, \tag{II-32}$$

and the beginning of the constant temperature epoch is taken at time t_i, corresponding to a scale factor $R(t_i) = R_1$. Similarly it can be shown that

$$f_V = \frac{1}{4(x-1)}\left[\tan^2\left\{\arctan(4x-1)^{1/2} + \frac{3\chi(t_i - t)}{2(x-1)^{1/2}}\right\} - 3\right], \tag{II-33}$$

Note that for $x = 2.971$ the scale factor increases by about 40 % during this constant temperature epoch.

2-4 Baryon Number Transport Across the Phase Boundary

The time variation of the baryon number densities, $n_B{}^q$ in QGP phase and $n_b{}^h$ in hadron gas phase, are described (Fuller, Mathews, & Alcock 1988) by

$$dn_b{}^q/dt = -\lambda n_b{}^q + \lambda' n_b{}^h - n_b{}^q[(dV/dt)/V + (df_V/dt)/f_V], \quad \text{(II-34)}$$

$$dn_b{}^h/dt = f_V/(1-f_V)[-\lambda' n_b{}^h + \lambda n_b{}^q + n_b{}^h(df_V/dt)/f_V] - n_b{}^h(dV/dt)/V, \quad \text{(II-35)}$$

$$n_b = f_V n_b^q - (1-f_V) n_b^h, \quad \text{(II-36)}$$

where the first and second source terms are the loss and gain terms for baryon transport across the phase boundary, and the $(dV/dt)/V$ and $(dfV/dt)/f_V$ terms are the red-shift and blue-shift factors for the expanding horizon volume and shrinking QGP volume. The horizon volume, V and the volume fraction of QGP, f_V are the solution, Eqs. (II-31) and (II-33).

The baryon permeability through the phase boundary was used in all previous studies from a simple classical argument, that is to assume an almost 100% absorption probability of baryon by QGP similarly to an absorption of an H_2O molecule by a water droplet. In order to improve this estimate by taking account of the quantum effects, we adopt (Sumiyoshi et al. 1989) the chromoelectric flux tube model (Casher, Neuberger & Nussinov 1979; Glendenning & Matsui 1983). Color electric field plays essential role in quark confinement. In this model, when a thermal quark passes through the phase boundary of QGP, a tube of color electric field is built behind it in the shortest distance, whose section is related to the QCD coupling constant, $\alpha_C = 2$. Mesons and baryons are respectively produced by virtual $q - \bar{q}$ and $qq - \bar{q}\bar{q}$ pair creation and fission of the tube (Sumiyoshi et al. 1989). Similarly to the $e^+ - e^-$ pair creation in QED, Schwinger

mechanism gives the probability, p, of the $q - \bar{q}$ pair creation and fission.

Let the magnitude of the transverse momentum of created virtual quark be by p_T. First we calculate the probability that each component of virtual pair will tunnel from the virtual state to a real state having the same energy as the original. The longitudinal momentum of each component at the point where the virtual pair first appears must satisfy

$$p_L^2 + p_T^2 + m^2 = 0. \tag{II-37}$$

As they move apart in the field of the tube their mutual interaction produces a field equal in magnitude but opposite in direction to the field in the tube. Thus, new field is destroying the origin field. After they have each moved a distance r in opposite directions from the point of first appearance, the energy balance reads

$$2\left[p_L^2(r) + p_T^2 + m^2\right]^{1/2} = 2k_{ST}r, \tag{II-38}$$

where k_{ST} is the energy per unit length stored in the flux tube. The action of both quarks integrated from the initial point to the point where they materialize given by $p_L(r) = 0$ is

$$S = 2\int_0^{E_T/k_{ST}} |p_L| dr = \frac{\pi E_T^2}{2k_{ST}}, \tag{II-39}$$

where $E_T = (p_T^2 + m^2)^{1/2}$. The probability that a virtual pair can tunnel to a real state in the field of the tube, with each component having transverse momentum p_T is therefore

$$P(p_T) = \exp(-\pi E_T^2/k_{ST}). \tag{II-40}$$

Now we con calculate the probability that a pair will actually be created. Following the Casher et al. (1979), we evaluate the vacuum persistence probability, which is the

probability that no such tunneling event for any spin, flavor, or transverse momentum has occurred at any r in the tube at any time t during the existence of the tube,

$$\begin{aligned}\langle 0_+ | 0_- \rangle^2 &= \prod_{flavor} \prod_{spin} \prod_{(\vec{p}_T)} \prod_{r} \prod_{t} [1 - P(p_T)] \\ &= \exp\left\{ \sum \sum \sum \sum \sum \ln [1 - P(p_T)] \right\}. \end{aligned} \tag{II-41}$$

Let $L_x L_y L_z T$ be the space time region of the tube in which no such event is supposed to have occurred. Let z be the longitudinal direction. Divide it into cells of length equal to that required for the materialization of a pair $\Delta z = 2E_T/k_{ST}$. The time interval T is divided into cells according to the frequency with which such tunneling attempts can occur in accordance with the uncertainty principle, $\Delta t = \pi/E_T$. Since $P(p_T)$ is independent of r, t, and spin, we obtain

$$\begin{aligned}\langle 0_+ | 0_- \rangle^2 &= \exp\left\{ 2 \frac{L_z}{\Delta z} \frac{T}{\Delta t} \sum_f \int \frac{p_T dp_T d\phi}{(2\pi/L_x)(2\pi/L_y)} \ln [1 - P(p_T)] \right\} \\ &= \exp - L_x L_y L_z T p(q - \bar{q}), \end{aligned} \tag{II-42}$$

where

$$p(q - \bar{q}) = \frac{k_{ST}^2}{4\pi^3} \sum_{flavor} \sum_{n=1}^{\infty} \frac{1}{n^2} \exp\left(- \frac{\pi m_f^2 n}{k_{ST}} \right). \tag{II-43}$$

The above $p(q-\bar{q})$ can be interpreted as a fission probability due to $q\bar{q}$ pair creation per unit four volume. In this equation m_f is the constituent quark mass of flavor f.

The string tension, k_{ST} depends on temperature, whose energy dependence is suggested

$$k_{ST}(T) = k_{ST}(0)[1 - T/T_c(1 - \delta)]^{0.42}, \tag{II-44}$$

with $\delta \approx 0.001$ from numerical simulation (Gao 1988) of QCD, where $k_{ST}(0)$ is set equal to 0.177GeV^2 deduced from the Regge trajectories of hadron mass spectrum. As to m_u, we adopted $m_u = 0.3$ GeV from our previous calculation (Suganuma, Kajino &

Yamamoto 1997) in the extended NJL model with quark confinement. However, the energy dependence of the constituent quark mass depends on models, and some model predicts $m_u \geq 0.1$ GeV also is likely at $T = T_c$. We therefore adopted m_u =0.1 GeV, too.

Since we do not know the masses of diquarks of any flavor or the mass of strange quark very precisely, the pair creation-fission probabilities for these quark(s)-pairs were taken from the analysis of high energy jet phenomenology (Andersson, Gustafson & Sjostrand 1982): $p(qq-\bar{q}q) : p(q-\bar{q}) = 0.065 : 1$, $p(u-\bar{u}) : p(d-\bar{d}) : p(s-\bar{s}) = 1 : 1 : 0.37$, and $p(uu-\bar{u}\bar{u}) : p(dd-\bar{d}\bar{d}) : p(ss-\bar{s}\bar{s}) = 1 : 0.058 : 0.0007$, where the sum over all different flavors is assumed in the first equation, and $q = u$ and d in the last equation. These probabilities explain the hadron fragmentation measured in high energy lepton and hadron collisions (Andersson, Gustafson & Sjostrand 1982) very well.

Having these probabilities p's, we can calculate (Sumiyoshi et al. 1989; Kajino et al. 1996) the flux of baryons evaporating from QGP at temperature T.

$$J_B = \sum_q \frac{n_q}{Z_q} \int d^3k_0 \exp(-\frac{E_0}{T}) \frac{k_{Z0}}{E_0} \int dk_Z{}^B \int dE^B \frac{1}{k_C{}^2} \exp[-\frac{E_0}{k_C{}^2}\{(k_{Z0} - k_Z{}^B) + \frac{1}{2E_{Z0}}((k_Z{}^B E_Z - k_{Z0}E_{Z0}) + m_q{}^2 \ln \frac{k_Z{}^B + E_Z}{k_{Z0} + E_{Z0}})\}], \quad \text{(II-45)}$$

where Z_q is the partition function, n_q is the quark number density, and E_0 is the thermal energy of an initial quark. k^B and E^B are the similar quantities for evaporating baryon. $k_C = \{3k_{ST}{}^3/2\pi\alpha_C p\}^{1/2}$ has a meaning of typical momentum which is lost before the baryon evaporation. Figure 3 displays the calculated $J_{B=p,n}$ normalized to the quark flux. Solid and dotted curves correspond to (m_q, M_B) = (0.3GeV, 0.94GeV) and (0.1GeV, 0.3GeV), respectively. Although the mass dependence is very strong, J_B is much smaller than J_q, suggesting that the baryon number is not easily transferred from QGP to hadron gas.

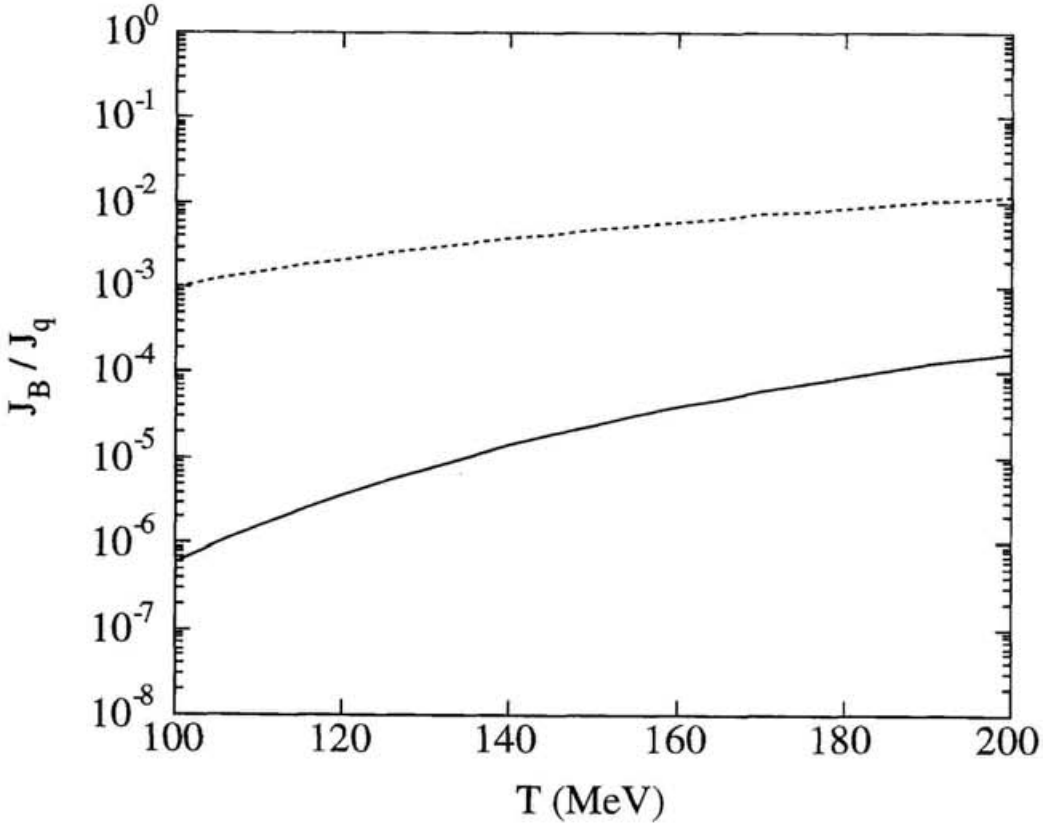

Figure 2-1: Flux of evaporating baryons from QGP normalized to the flux of thermal quarks. Solid and dotted curves correspond to (m_q, M_B) = (0.3GeV, 0.94GeV) and (0.1GeV, 0.3GeV)

The baryon penetration factors $\lambda {n_B}^q$ and $\lambda' {n_B}^h$ in Eqs. (II-34) and (II-35) are thus given (Sumiyoshi, Kajino, Alcock & Mathews 1990) by

$$\lambda {n_b}^q = 4\pi r(t)^2 \cdot N_{NUC}\{V(t_c)/V(t)f_V(t)\}J_B {n_b}^q(t)/{n_b}^q(t_c), \quad \text{(II-46)}$$

$$\lambda' {n_b}^h = 4\pi r(t)^2 \cdot N_{NUC}\{V(t_c)/V(t)f_V(t)\}J_B {n_b}^h(t)/{n_b}^h(t_c), \quad \text{(II-47)}$$

where $J_Q(T_c)$ is the flux of leading quark, $J_B(T_c)$ is given by Eq. (9), N_{NUC} is calculated in Eq. (4), and $r(t) = (3/4\pi \cdot (1 - f_V(t))V(t)/N_{NUC}V(t_c))^{1/3}$ is the average bubble radius.

Having known all source terms, we can now solve the coupled differential Eqs. (II-34) and (II-35). The numerical solution (Kajino et al. 1996) of these equations is displayed in Fig. 2-2 for the QCD parameters $T_C = 150$ MeV and $\sigma = 10^6$ MeV^3, where $R = {n_B}^q/{n_B}^h$. If the whole system is in the statistical equilibrium, both ${n_B}^q$ and ${n_B}^h$ stay at the initial values, and hence R being constant ≈ 100. It is a common misconception in many papers (Witten 1984) that the most natural baryon density contrast is such a thermodynamic ratio as $R \approx 100$ in chemical and statistical equilibrium. Fig. 2-2 shows clearly that the baryon transport is a strongly non-equilibrium process. Especially, near the end of the phase transition, the transport of baryon number across the phase boundary cannot be efficient enough to establish complete chemical equilibrium because the velocity of the phase boundary continuously increases. We define (Sumiyoshi, Kajino, Alcock & Mathews 1990) the end of the phase transition at which the speed of the boundary approaches the sound velocity of relativistic plasma $V_S = c/\sqrt{3}$. After this time the QGP droplets lose energy source from the latent heat and dive again into the supercooling phase, from which the high baryon-number density zones with finite volume fraction emerge promptly. The resultant density contrast is very huge, $R \gtrsim 10^4$.

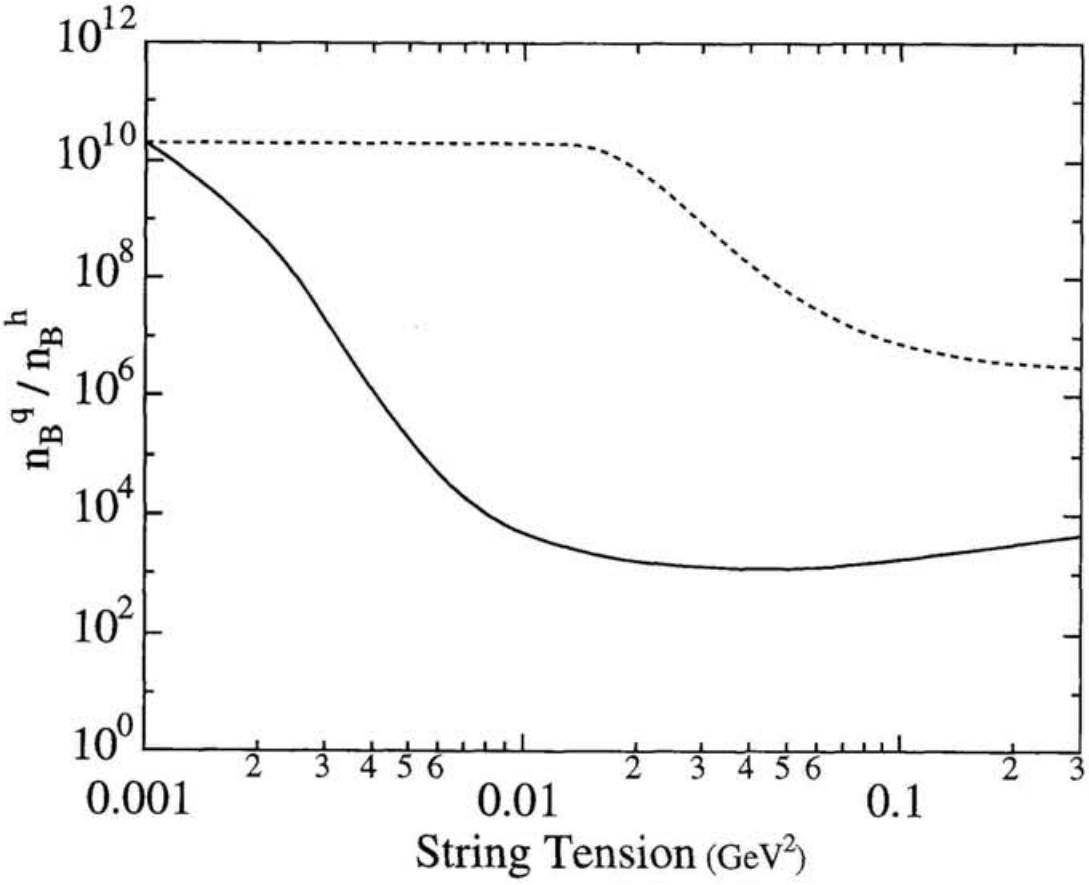

Figure 2-2: Ratio of the baryon-number density in QGP to the baryon-number density in hadron gas, versus string tension at end of phase transition. Dotted and Solid curves correspond to (m_q, M_B) = (0.3GeV, 0.94GeV) and (0.1GeV, 0.3GeV)

§3 Primordial Nucleosynthesis and Constraints on Ω_b

3-1 Homogeneous Big-Bang Nucleosynthesis

The analysis of primordial nucleosynthesis provides valuable limits on cosmological and particle physics parameters through a comparison between the predicted and inferred primordial abundances of D, ^{3}He, ^{4}He, and ^{7}Li. For standard homogeneous big bang nucleosynthesis (HBBN) the predicted primordial abundances of these light-elements are in accord with the value inferred from observation provided that baryon-to-photon ratio ($\equiv \eta$) is between about 2.5×10^{-10} and 6×10^{-10}. This corresponds to an allowed range for the baryon fraction of the universal closure density ${\Omega_b}^{\rm HBBN}$ (Wagoner, Fowler, & Hoyle 1967; Wagoner 1973; Walker et al. 1991; Smith, Kawano, & Malaney 1993; Copi, Schramm & Turner 1995; Schramm & Mathews 1995),

$$0.04 \lesssim {\Omega_b}^{\rm HBBN}\, h_{50}^2 \lesssim 0.08, \qquad \text{(III-1)}$$

where $\eta = 6.6 \times 10^{-9} \Omega_b\, h_{50}^2$. The lower limit on ${\Omega_b}^{\rm HBBN}$ arises mainly from the upper limit on the deuterium plus ^{3}He abundance (Yang et al. 1984; Walker et al. 1991; Smith, Kawano, & Malaney 1993), and the upper limit to Ω_b arises from the upper limit on the ^{4}He mass fraction $Y_{\rm p}$ and/or the deuterium abundance D/H $\geq 1.2 \times 10^{-5}$ (Linsky et al. 1993, 1995). Here, h_{50} is the Hubble constant in units of 50 km s $^{-1}$ Mpc^{-1}. The fact that this range for $\Omega_b\, h_{50}^2$ is so much greater than the current upper limit to the contribution from luminous matter ${\Omega_b}^{Lum} \lesssim 0.01$ (see however Jedamzik, Mathews & Fuller 1995) is one of the strongest arguments for the existence of baryonic dark matter.

Over the years HBBN has provided strong support for the standard, hot big bang cosmological model as mentioned above. However, as the astronomical data have become more precise in recent years, a possible conflict between the predicted abundances of the light element isotopes from HBBN and the abundances inferred from observations

has been suggested (Olive & Steigman 1995; Steigman 1996a; Turner et al. 1996; Hata et al. 1996; see also Hata et al. 1995).

There is now a good collection of abundance information on the ^{4}He mass fraction, $Y_{\rm p}$, O/H, and N/H in over 50 extragalactic HII regions (Pagel et al. 1992; Pagel 1993; Izatov, Thuan & Lipovetsky 1994; Skillman & Kennicutt 1995). In an extensive study based upon these observations, the upper limit to η from the observed ^{4}He abundance was found to be $\sim 3.5 \times 10^{-10}$ (Olive & Steigman 1995; Olive & Scully 1996) when a systematic error in $Y_{\rm p}$ of $\Delta Y_{sys} = 0.005$ is adopted. Recently, it has been recognized that the ΔY_{sys} may even be factor of 2 or 3 larger (Thuan,, Nature, Izatov, &Lipovetsky 1996; Copi, Schramm & Turner 1995; Schramm & Mathews 1995; Sasselov & Goldwirth 1995), making the upper limit to η as large as 7×10^{-10}.

On the other hand, the lower bound to η has been derived directly from the upper bound to the combined abundances of D and ^{3}He. This is because it is believed that deuterium is largely converted into ^{3}He in stars; the lower bound then applies if, as has generally been assumed, a significant fraction of ^{3}He survives stellar processing (Walker et al. 1991).

However, there is mounting evidence that low mass stars destroy ^{3}He (Wasserburg, Boothroyd & Sackmann al 1995; Charbonnel 1995), although it is possible that massive stars produce ^{3}He. Therefore, the uncertainties of chemical evolution models render it difficult to infer the primordial deuterium and ^{3}He abundances by using observations of the present interstellar medium (ISM) or from the solar meteoritic abundances. Recent data and analysis lead to a lower bound of $\eta \gtrsim 3.5 \times 10^{-10}$ on the basis of D and ^{3}He (Dearborn, Steigman, & Tosi 1996; Hata et al. 1996; Steigman 1996a; Steigman & Tosi 1995), if the fraction of ^{3}He that survives stellar processing in the course of galactic evolution exceeds 1/4 (Dearborn, Schramm, & Steigman 1986). This poses a potential

conflict between the observation ($Y_{\rm p}$ with low ΔY_{sys}, D) and HBBN.

With this in mind, it is worthwhile to consider alternative cosmological models. One of the most widely investigated possibilities is that of an inhomogeneous density distribution at the time of nucleosynthesis. Such studies were initially motivated by speculation (Witten 1984; Applegate & Hogan 1985) that a first order quark-hadron phase transition (at $T \sim 100\,{\rm MeV}$) could produce baryon inhomogeneities as baryon number was trapped within bubbles of shrinking quark-gluon plasma. In previous calculations using the baryon inhomogeneous big bang nucleosynthesis (IBBN) model, it has been usually assumed that the geometry of baryon density fluctuations is approximated by condensed spheres. Such geometry might be expected to result from a first order QCD phase transition in the limit that the surface tension dominated the evolution of shrinking bubbles of quark-gluon plasma. However, the surface tension may not be large (Kajantie, Kärkkäinen & Rummukainen 1990, 1991, 1992) during the QCD transition, which could lead to a "shell" geometry or the development of dendritic fingers (Freese & Adams 1990). Furthermore, such fluctuations might have been produced by a number of other processes operating in the early universe (cf. Malaney & Mathews 1993), for which other geometries may be appropriate, e.g. strings, sheets, etc. Thus, the shapes of any cosmological baryon inhomogeneities must be regarded as uncertain.

The purpose of this section is, therefore, to explore the sensitivity of the predicted elemental abundances in IBBN models to the geometry of the fluctuations. We consider here various structures and profiles for the fluctuations in addition to condensed spheres. Mathews et al. (1990, 1994, 1996) found that placing the fluctuations in spherical shells rather than condensed spheres allowed for lower calculated abundances of ^{4}He and ^{7}Li for the same Ω_b, and that a condensed spherical geometry is not necessarily the optimum. Here we show that a cylindrical geometry also allows for an even higher

baryonic contribution to the closure density than that allowed by the usually adopted condensed sphere. It appears to be a general result that shell geometries allow for a slightly higher baryon density. This we attribute to the fact that, for optimum parameters, shell geometries involve a larger surface area to volume ratio and hence more efficient neutron diffusion.

An important possible consequence of baryon inhomogeneities at the time of nucleosynthesis may be the existence of unique nucleosynthetic signatures. Among the possible observable signatures of baryon inhomogeneities already pointed out in previous works are the high abundances of heavier elements such as beryllium and boron (Boyd & Kajino 1989; Kajino & Boyd 1990; Malaney & Fowler 1989; Terasawa & Sato 1990; Kawano et al. 1991), intermediate mass elements (Kajino, Mathews & Fuller 1990), or heavy elements (Malaney & Fowler 1988; Applegate, Hogan & Scherrer 1988; Rauscher et al. 1994). Such possible signatures are also constrained, however, by the light-element abundances. It was found in several previous calculations that the possible abundances of synthesized heavier nuclei was quite small (e.g., Alcock et al. 1990; Terasawa & Sato 1990; Rauscher et al. 1994). We find, however, that substantial production of heavier elements may nevertheless be possible in IBBN models with cylindrical geometry.

3-2 Baryon Density Inhomogeneities

After the initial suggestion (Witten 1985) of QCD motivated baryon inhomogeneities it was quickly realized (Applegate & Hogan 1985; Applegate, Hogan & Scherrer 1987) that the abundances of primordial nucleosynthesis could be affected. A number of pa-

pers have addressed this point (Alcock, Fuller, & Mathews 1987; Applegate, Hogan & Scherrer 1987, 1988; Fuller, Mathews, & Alcock 1988; Kurki-Suonio et al. 1988, 1990; Terasawa & Sato 1989a, b, c, 1990; Kurki-Suonio & Matzner 1989, 1990; Mathews et al. 1990, Mathews, Schramm & Meyer 1993; Mathews, Kajino & Orito 1996; Jedamzik, Fuller & Mathews 1994; Jedamzik, Mathews & Fuller 1995; Thomas et al. 1994; Rauscher et al. 1994). Most recent studies in which the coupling between the baryon diffusion and nucleosynthesis has been properly accounted for (e.g., Terasawa & Sato 1989a, b, c, 1990; Kurki-Suonio & Matzner 1989, 1990; Mathews et al. 1990, Mathews, Schramm & Meyer 1993; Jedamzik, Fuller & Mathews 1994; Thomas et al. 1994) have concluded that the upper limit on $\Omega_b h^2$ is virtually unchanged when compared to the upper limit on $\Omega_b h^2$ derived from standard HBBN. It is also generally believed (e.g. Vangioni-Flam & Casse 1995) that the same holds true if the new high D/H abundance is adopted.

However, in the previous studies, it was usually assumed that a fluctuation geometry of centrally condensed spheres produces the maximal impact on nucleosynthesis. Here we emphasize that condensed spheres are not necessarily the optimal nor the most physically motivated fluctuation geometry.

Several recent lattice QCD calculations (Kajantie, Kärkkäinen & Rummukainen 1990, 1991, 1992; Brower et al. 1992) indicate that the surface tension of nucleated hadron bubbles is relatively low. In this case, after the hadron bubbles have percolated, the structure of the regions remaining in the quark phase may not form spherical droplets but rather sheets or filaments. We do note that the significant effects on nucleosynthesis may require a relatively strong first order phase transition and sufficient surface tension to generate an optimum separation distance between baryon fluctuations (Fuller, Mathews, & Alcock 1988). However, even if the surface tension is low,

the dynamics of the coalescence of hadron droplets may lead to a large separation between regions of shrinking quark-gluon plasma. Furthermore, even though lattice QCD has not provided convincing evidence for a strongly first order QCD phase transition (e.g., Fukugita & Hogan 1991), the order of the transition must still be considered as uncertain (Gottlieb 1991; Petersson 1993). It depends sensitively upon the number of light quark flavors. The transition is first order for three or more light flavors and second order for two. Because the s quark mass is so close to the transition temperature, it has been difficult to determine the order of transition. At least two recent calculations (Iwasaki et al. 1995; Kanaya 1996) indicate a clear signature of a first order transition when realistic u, d, s quark masses are included, but others indicate either second order or no phase transition at all.

In addition to the QCD phase transition, there remain a number of alternative mechanisms for generating baryon inhomogeneities prior to the nucleosynthesis epoch (cf. Malaney & Mathews 1993), such as electroweak baryogenesis (Fuller et al. 1994), inflation-generated isocurvature fluctuations (Dolgov & Silk 1993), and kaon condensation (Nelson 1990). Cosmic strings might also induce baryon inhomogeneities through electromagnetic (Malaney & Butler 1989) or gravitational interactions.

Since the structures, shapes, and origin of any baryon inhomogeneities are uncertain, a condensed spherical geometry is not necessarily the most physically motivated choice. Indeed, we will show that a condensed spherical geometry is also not necessarily the optimum to allow for the highest values for Ω_b while still satisfying the light-element abundance constraints. Here we consider the previously unexplored cylindrical geometry. String geometries may naturally result from various baryogenesis scenarios such as superconducting axion strings or cosmic strings. Also, the fact that QCD is a string theory may predispose QCD-generated fluctuations to string-like geometry (Kajino &

Tessie 1993; Tassie & Kajino 1993). Hence, cylindrical fluctuations may be a natural choice.

3-3 Observational Constraints for Light Element Abundances

We adopt the following constraints on the observed helium mass fraction Y_p and ^{7}Li taken from Balbes et al. (1993), Schramm & Mathews (1995), Copi et al. (1995) and Olive (1996):

$$0.226 \leq Y_{\rm p} \leq 0.247, \tag{III-2}$$

$$0.7 \times 10^{-10} \leq {}^7{\rm Li/H} \leq 3.5 \times 10^{-10}. \tag{III-3}$$

i) Helium Constraints

The current status of ^{4}He observations and potential systematic errors have been recently reviewed Skillman et al. 1994, Schramm & Mathews 1995. The primordial helium abundance is generally inferred from the correlation of helium abundance with metallicity in the HII regions of compact blue irregular galaxies. The random errors in the correlation of helium with metallicity are very small due to multiple exposures, several standard stars, and good linear detectors. In principle, it is possible to obtain line ratios which are accurate to within 2% (Skillman et al. 1994). There is, however, a need more high quality observations at low [O/H]. Also it is not know whether there are deviations a linear regression at low metallicity. Such deviations might be expected from galactic chemical evolution models Mathews, Boyd & Fuller 1993, Mathews, Schramm

& Meyer 1993, Balbes et al. (1993), Pagel 1993. Most importantly, the uncertainties in theoretical recombination/cascade calculations are not well quantified.

Based upon an analysis Olive & Steigman 1995 of preliminary data from Skillman, the presently inferred primordial value is $Y_p = 0.232$, with a statistical uncertainty of ± 0.003, and possible systematic errors as much as $\pm^{0.01}_{0.005}$. This implies an upper limit of 0.247 to the primordial helium abundance which is adopted here as in other recent reviews Copi, Schramm & Turner 1995, Schramm & Mathews 1995. This primordial ^{4}He abundance constraint includes a statistical uncertainty of ± 0.003 and possible systematic errors as much as $+0.01/-0.005$ with central value of 0.234. A recent reinvestigation (with new data) of the linear regression method for estimating the primordial ^{4}He abundance has called into question the systematic uncertainties assigned to $Y_{\rm p}$ (Izatov, Thuan & Lipovetsky 1996). Our adopted upper limit to $Y_{\rm p}$ of Eq. (III-2) is essentially equal to the limit derived in their study with 1σ statistical error.

ii) Lithium Constraints A number of different values for the upper limit to the primordial lithium abundance have been adopted in the literature. It is, therefore, worthwhile to say a few words about them. It is convention in the literature to quote the lithium abundance relative to H = 10^{12}. Hence, one defines a quantity [Li] = 12 + log(Li/H). One recently adopted primordial lithium abundance constraint Walker et al. 1991 [also used in Thomas et al. (1994)] is [Li] ≤ 2.15 (Li/H $\leq 1.4 \times 10^{-10}$). This limit is based upon a weighted mean of observations of 35 low metallicity halo stars with $T_{eff} \geq 5500$ K on the so called "lithium plateau" Spite & Spite 1982. A limit of [Li] ≤ 2.15 corresponds to the 2σ confidence limit above the mean value of 2.08.

This upper limit was motivated somewhat by the standard main sequence models of Deliyannis et al. 1990 which imply little lithium depletion in low metallicity halo stars.

However, even in Deliyannis et al. 1990 it was pointed out that a higher limit to primordial lithium is more appropriate. By adopting conservative errors in abundance determinations for both cool and hot stars, and directly fitting a series of isochronous to the data, they obtained a 2σ upper limit of [Li] $\leq$ 2.21. Including effects of diffusion into their stellar evolution code, increases this upper limit to [Li] $\leq$ 2.36. This is the limit adopted in Smith et al. (1993). It represents the most conservative application of the Deliyannis et al. 1990 results. One important development since that limit was adopted is a reanalysis Thorburn. 1994 of the model atmospheres used to infer the lithium abundance which shifts [Li] upward by 0.2. These data also indicate systematic variations in the lithium abundance with surface temperature, possibly indicating that some depletion has occurred. We also note another recent discussion of model atmospheres Kurucz 1995 which suggests that as much as an order of magnitude upward shift in the primordial lithium abundance could be warranted due to the tendency of one-dimensional models to under estimate the ionization of lithium.

Related to the above it is also worth noting that when effects of rotational mixing have been added to stellar models Pinsonneault, Deliyannis & Demarque 1992 for lithium depletion, a much larger lithium depletion seems possible. This factor is largely independent of initial rotation for low metallicity stars. Furthermore, the predicted metallicity dependence of the dispersion in lithium depletion with rotation may even be necessary to account for the dispersion in the observed plateau lithium abundances. It is also noted in Pinsonneault, Deliyannis & Demarque 1992 that the rotational models with the same set of parameters and physical assumptions are capable of reproducing the very different lithium depletion patterns observed in both metal poor halo stars

and population I stars in the disk which exhibit much greater lithium depletion and dispersion. This is a powerful argument for the validity of the rotational mixing models which should, perhaps, be taken seriously.

An objection to the possible large depletion factor for lithium, however, stems from recent possible detections Smith, Lambert & Nissen 1992, Hobbs & Thorburn 1994 of ^{6}Li in two of the plateau halo stars. Since ^{6}Li should be destroyed much more rapidly than ^{7}Li Brown & Schramm 1988, the presence of ^{6}Li argues against significant ^{7}Li destruction. On the other hand, the ^{6}Li detection is still consistent with as much as a factor of two ^{7}Li destruction (Copi et al. 1995b). Furthermore, it is possible Yoshii, Mathews, & Kajino 1995 that some of the ^{6}Li is the result of more recent accretion of interstellar material which could occur as halo stars episodically plunge through the disk. Such a process could mask the earlier destruction of lithium. A possible way to distinguishing between accreted and primordial material might be the detections of a B/Be ratio which is consistent with IBBN or HBBN rather than the cosmic-ray ratio. The IBBN B/Be ratio from these calculations is discussed separately in Yoshii et al. (1995).

In view of the above discussion, it is our opinion, that the most realistic upper limit to the lithium abundance is probably that adopted in Copi et al. (1995b), i.e. Li/H $\leq 3.5 \times 10^{-10}$. This limit includes the systematic increase from the model atmospheres of Thorburn (1994) and the possibility of as much as a factor of 2 increase due to stellar destruction (consistent with the ^{6}Li observations. This is the limit which we adopt here. For comparison, however, the most extreme conservative upper limit to the lithium abundance is probably that derived from the fits to the data by Pinsonneault et al. (1992) based upon models in which rotational mixing has been included. Using a fit their isochronous to the lithium plateau, they obtained an upper limit on the primordial

population II lithium abundance of

$$^7\mathrm{Li/H} < 1.5 \times 10^{-9}. \qquad \text{(III-4)}$$

We also show results from this more conservative upper limit, with the caveat that this limit may not be consistent with the observed ^{6}Li abundance.

iii). Deuterium and ^{3}He Constraints

The primordial abundance of deuterium is even harder to clarify since it is easily destroyed in stars (at temperatures exceeding about 6×10^5K). Previously, limits on the deuterium (and also the ^{3}He) abundances have been inferred from their presence in presolar material (e.g., Walker et al. 1991). It is also inferred from the detection in the local interstellar medium (ISM) through its ultraviolet absorption lines in stellar spectra but, as expected for a fragile element, its abundance shows a large scatter, $\mathrm{D/H} \approx (0.2-4) \times 10^{-5}$, suggesting localized abundance fluctuations and/or systematic errors. McCullough (McCullough 1992) finds that after discarding some unreliable measurements, the 7 *IUE* and 14 *Copernicus* measurements along the cleanest lines of sight (towards hot stars within about 1 kpc) are all consistent with an interstellar abundance of $\mathrm{D/H} = 1.5 \pm 0.2 \times 10^{-5}$.

Recently the *HST* has provided a more accurate measurement of $\mathrm{D/H} = 1.60 \pm 0.09\,(\mathrm{stat})^{+0.05}_{-0.10}\,(\mathrm{syst}) \times 10^{-5}$ towards the star *Capella* at 12.5 kpc.(Linsky et al. 1993; 1995) However since the Lyman-α line (of hydrogen) is severely saturated even towards such a nearby star, such observations, although precise, cannot test whether there are real spatial variations in the interstellar deuterium abundance. It has been argued Epstein et al. 1976 that there are no important astrophysical sources of deuterium

and observational attempts to detect signs of deuterium synthesis in the Galaxy have so far not contradicted this belief (see Pasachoff & Vidal-Madjar 1989). Then the lowest D abundance observed today provides a reliable lower bound to the primordial abundance. If this is indeed so, then the lowest D abundance observed today should provide a lower bound to the primordial abundance. Recent precise measurements by Linsky et al. (1995, 1993) using the *Hubble Space Telescope* implies

$$\mathrm{D/H} > 1.2 \times 10^{-5}. \tag{III-5}$$

There are similar large fluctuations in the abundance of ^{3}He which has been detected through its radio recombination line in a dozen galactic H II regions. The values measured by Balser et al. (1994) range over

$$\left(\frac{^3\mathrm{He}}{\mathrm{H}}\right)_{\mathrm{H\,II}} \sim (1-4) \times 10^{-5}\ . \tag{III-6}$$

It has also been detected (Rood, Bania & Wilson 1992) with a large abundance (^{3}He/H $\approx$ 10^{-3}) in the planetary nebula NGC3242, in accord with the theoretical expectation (Dearborn, Schramm, & Steigman 1986) that it is created in low mass stars. However the galactic observations find the highest ^{3}He abundances in the outer Galaxy where stellar activity is *less* than in the inner Galaxy. While regions with high abundances do lie preferentially in the Perseus spiral arm, there are large source-to-source variations which do not correlate with stellar activity. (Balser et al. 1994) Thus these measurements do not provide any reliable cosmological input.

Yang et al. (1994) had suggested that the uncertainties in determining the primordial abundances of D and ^{3}He may circumvented by considering their *sum*. They argued that since D is burnt in stars to ^{3}He, a fraction g_3 of which survives stellar processing, the primordial abundances may be related to the abundances later in time through the

inequality

$$\left(\frac{\mathrm{D}+{}^3\mathrm{He}}{\mathrm{H}}\right)_{\mathrm{p}} < \left(\frac{\mathrm{D}+{}^3\mathrm{He}}{\mathrm{H}}\right) + \left(\frac{1}{g_3}-1\right)\left(\frac{{}^3\mathrm{He}}{\mathrm{H}}\right) \ . \qquad \text{(III-7)}$$

As reviewed by Geiss (1993) the terms on the rhs may be determined at the time of formation of the Solar system, 4.6 Gyr ago. The abundance of ^{3}He in the Solar wind, deduced from studies of gas-rich meteorites, lunar rocks and metal foils exposed on lunar missions, may be identified with the sum of the pre-Solar abundances of ^{3}He and D (which was burnt to ^{3}He in the Sun), while the smallest ^{3}He abundance found in carbonaceous chondrites, which are believed to reflect the composition of the pre-Solar nebula, may be identified with the pre-Solar abundance of ^{3}He alone. For example, Walker et al. (1991) obtained

$$1.3\times10^{-5} \lesssim \left(\frac{{}^3\mathrm{He}}{\mathrm{H}}\right)_{\odot} \lesssim 1.8\times10^{-5}\ , \quad 3.3\times10^{-5} \lesssim \left(\frac{\mathrm{D}+{}^3\mathrm{He}}{\mathrm{H}}\right)_{\odot} \lesssim 4.9\times10^{-5}. \qquad \text{(III-8)}$$

By using a closed-box instantaneous recycling approximation, it is straightforward (Olive et al. 1990) to show that the sum of primordial deuterium and ^{3}He can be written

$$y_{23p} \leq A_{\odot}^{(g_3-1)} y_{23\odot}\left(\frac{X_{\odot}}{X_p}\right) \qquad \text{(III-9)}$$

where $A_{\odot}$ is the fraction of the initial primordial deuterium still present when the solar system formed, g_3 is the fraction of ^{3}He that survives incorporation into a single generation of stars, $y_{23\odot}$ is the presolar value of [D+^{3}He]/H inferred from the gas rich meteorites, and $X_{\odot}/X_p$ is the ratio of the presolar hydrogen mass fraction to the primordial value. These factors together imply an upper limit (Walker et al. 1991; Copi, Schramm & Turner 1995) of

$$y_{23p} \leq 1.1 \times 10^{-4}. \qquad \text{(III-10)}$$

There are however several reasons to distrust the above bound, from which a stringent lower limit on η has been deduced. First, it is not clear if the Solar system

abundances provide a representative measure at all, given that observations of ^{3}He elsewhere in the Galaxy reveal unexplained source-to-source variations. Indeed the pre-Solar abundance of ^{3}He is *less* than some of the present day interstellar values. Second, the survival fraction of ^{3}He may have been overestimated since there may be net *destruction* of ^{3}He in low mass stars through the same mixing process which appears to be needed to explain other observations, e.g. the $^{12}C/^{13}C$ ratio (Hogan 1995). In fact a recent measurement using *Ulysses* finds that $^3He/^4He = 2.2^{+0.7}_{-0.6}\,(\mathrm{stat}) \pm 0.2\,(\mathrm{syst}) \times 10^{-4}$ in the local interstellar cloud, rather close to the value of $1.5 \pm 0.3 \times 10^{-4}$ in the pre-solar nebula, demonstrating that the ^{3}He abundance has hardly increased since the formation of the Solar system (Gloeckler & Geiss 1996).

It is obviously crucial to detect deuterium outside the Solar system and the nearby interstellar medium in order to get at its primordial abundance and also, of course, to establish its cosmological origin. Astronomers have attempted to measure Lyman-series absorption lines of deuterium in the spectra of distant quasars, due to foreground intergalactic clouds made of primordial unprocessed material. Problems arise in studying such quasar absorption systems (QAS) because of possible confusion with neighboring absorption lines of hydrogen and multi-component velocity structure in the clouds.

Possible detections (Songaila et al. 1994; Carswell et al. 1994; 1996; Tytler & Fan 1994; Tytler, Fan, & Burlers 1996; Rugers & Hogan 1996a,1996b; Wampler et al. 1996) of an isotope-shifted Lyman-α absorption line at high redshift ($z \gtrsim 3$) along the line of sight to quasars are of considerable interest. Quasar absorption systems can sample low metallicity gas at early epochs where little destruction of D should have occurred. Thus, they should give definitive measurements of the primordial cosmological D abundance. A very recent high resolution detection by Rugers & Hogan (1996a) suggests a ratio

D/H of

$$\mathrm{D/H} = 1.9 \pm 0.4 \times 10^{-4}. \qquad \text{(III-11)}$$

This result is consistent with the estimates made by Songaila et al. (1994) and Carswell et al. (1994), using lower resolution (but see, Tytler, Burlers, & Kirkman 1997). It is also similar to that found recently in another absorption system by Wampler et al. (1996), but it is inconsistent with high resolution studies in other systems at high redshift (Tytler, Fan & Burles 1996; Burles & Tytler 1996) and with the local observations of D and ^{3}He in the context of conventional models of stellar and Galactic evolution (Edmunds 1994; Gloeckler & Geiss 1996). If the high value of D/H is taken to be the primordial abundance, then the consistency between the observation and HBBN is recovered and the allowed range of Ω_b inferred from HBBN changes to ${\Omega_b}^{\mathrm{HBBN}} h_{50}^2 = 0.024 \pm 0.002$ (Jedamzik, Fuller & Mathews 1994; Krauss & Kernan 1994; Vangioni-Flam & Casse 1995). In this case, particularly if h_{50} is greater than ~ 1.5, the big bang prediction could be so close to the baryonic density in luminous matter that little or no baryonic dark matter is required (Persic & Salucci 1992; Jedamzik, Mathews & Fuller 1995). This could be in contradiction with observation, particularly if the recently detected microlensing events (Alcock et al. 1993, 1994, 1995abc; Aubourg et al. 1993) are shown to be baryonic. This low baryonic density limit would also be contrary to evidence (White et al. 1993; White and Fabian 1995) that baryons in the form of hot X-ray gas may contribute a significant fraction of the closure density

The observations by Tytler, et al. (1996) and Burles & Tytler (1996) yield a low value of D/H. Their average abundance is

$$\mathrm{D/H} = 2.4 \pm 0.9 \times 10^{-5}, \qquad \text{(III-12)}$$

with $\pm 2\sigma$ statistical error and $\pm 1\sigma$ systematic error. This value is consistent with the expectations of local galactic chemical evolution. However, this value would imply an

HBBN helium abundance of $Y_p = 0.249 \pm 0.003$ which is only marginally consistent with the observationally inferred Y_p even if the high ΔY_{sys} is adopted.

We adopt Eq. III-5 as a lower limit to the primordial deuterium abundance for the purposes of exploring the maximal cosmological impact from IBBN. In addition, we consider the two possible detections of the deuterium abundance along the line of sight to high red shifted quasars, Eqs. (III-11) and (III-12) as possible limits.

3-4 Calculational Method

The calculations described here are based upon the coupled diffusion and nucleosynthesis code of Mathews et al. (1990), but with a number of nuclear reaction rates updated and the numerical diffusion scheme modified to accommodate cylindrical geometry. We also have implemented an improved numerical scheme which gives a more accurate description of the effects of proton and ion diffusion, and Compton drag at late times. Although our approach is not as sophisticated as that of Jedamzik et al. (1994a), it produces essentially the same results for the parameters employed here. We have also included all of the new nuclear reaction rates summarized in Smith et al. (1993) as well as those given in Thomas et al. (1993). We obtain the same result as Smith et al. (1993) using these rates and homogeneous conditions in our IBBN model

Calculations were performed in a cylindrical geometry both with the high density regions in the center (condensed cylinders), and with the high density regions in the outer zone of computation (cylindrical shells). Similarly, calculations were made in a spherical geometry with the high density regions in the center (condensed spheres) and

with the high density region in the outer zones of computation (spherical shells).

In the calculations, the fluctuations are resolved into 16 zones of variable width as described by Mathews et al. (1990). We assumed three neutrino flavors and an initially homogeneous density within the fluctuations. Such fluctuation shapes are the most likely to emerge, for example, after neutrino-induced expansion (Jedamzik & Fuller 1994). We use a neutron mean life-time of $\tau_n = 887.0$ (Particle Data Group 1994). In addition to the cosmological parameter, Ω_b and fluctuation geometry, there remain three parameters to specify the baryon inhomogeneity. They are: R, the density contrast between the high and low-density regions; f_v, the volume fraction of the high-density region; and r, the average separation distance between fluctuations.

3-5 Numerical Results and Discussions

The parameters R and f_v were optimized to allow for the highest values for $\Omega_b\, h_{50}^2$ while still satisfying the light-element abundance constraints. For fluctuations represented by condensed spheres, optimum parameters are $R \sim 10^6$ and $f_v^{1/3} \sim 0.5$ (Mathews, Kajino & Orito 1996). For other fluctuation geometries, we have found that optimum parameters are:

$$R \sim 10^6; \qquad \text{for all fluctuation geometries}$$

$$f_v^{1/3} \sim \begin{cases} 0.5; & \text{for condensed spheres} \\ 0.19; & \text{for spherical shells,} \end{cases}$$

$$f_v^{1/2} \sim \begin{cases} 0.5; & \text{for condensed cylinders} \\ 0.15; & \text{for cylindrical shells,} \end{cases}$$

although there is not much sensitivity to R once

$R \gtrsim 10^3$. Regarding f_v, we have written the appropriate length scale of high density regions, i.e. $f_v^{1/3}$ and $f_v^{1/2}$ for the spherical and cylindrical fluctuation geometries, respectively. The variable parameters in the calculation are then the fluctuation cell radius r, and the total baryon-to-photon ratio η (or $\Omega_b\, h_{50}^2$).

3-6 Constraints on $\Omega_b\, h_{50}^2$

Figures 3-1 shows contours of allowed parameters in the r vs. η and r vs. $\Omega_b h_{50}^2$ plane for condensed sphere fluctuations for the adopted light-element abundance constraints (Copi et al. 1995b). The fluctuation cell radius r is given in units of meters for a comoving length scale fixed at a temperature of $kT = 1$ MeV. The limits from various light-element abundance constraints (including both possible ^{7}Li limits) as discussed above are drawn as indicated.

Also, for illustration, Figure 3-3 shows the same contour plots for a possible high Lyman-α D/H and [D + ^{3}He]/H constraint. Figures 3-2 show the same contours for a spherical shell geometry. As in previous calculations Mathews et al. 1990 the shell geometry models (shown in Figures 3-2) produce a slightly lower helium and lithium abundance than the condensed sphere geometry for the same value of $\Omega_b h_{50}^2$. One additional advantage of the spherical shell geometry is that the yields are largely independent of the fluctuation separation distance, which decreases the sensitivity of the calculation to that unknown parameter.

Some points to note from figures 3-1 and 3-2 that with the presently adopted primordial light-element abundances, the upper limits to η and $\Omega_b h_{50}^2$ are now largely determined from D/H and ^{7}Li for condensed sphere geometry, but by Y_p and ^{7}Li for spherical shells; 2) the range of allowable values for the baryon density are comparable to HBBN for small separation distances r, but there remain regions of the parameter space with optimum separation distances at which significantly higher values for η or $\Omega_b h_{50}^2$ are allowed. This is true even for a high deuterium abundance; and 3) These limits can be increased even further if a higher (population I) primordial ^{7}Li abundance limit is adopted as some have proposed.

The optimum separation distance in each case roughly corresponds to a neutron diffusion length during nucleosynthesis Mathews et al. 1990. Allowing for this possibility increases the maximum allowable values of the baryonic contribution to the closure density to $\Omega_b h_{50}^2 \leq 0.11$ ($\eta \leq 7 \times 10^{-10}$) for the spherical shell geometry and the adopted limits. The condensed sphere limits, however are unchanged from the HBBN model. On the other hand, if the primordial ^{7}Li abundance could be as high as Li/H $\leq 1.3 \times 10^{-9}$, then the upper limits for and condensed sphere geometry could be as high as $\Omega_b h_{50}^2 \leq 0.13$ ($\eta \leq 8.6 \times 10^{-10}$) with similar values for the spherical shells. With a possible high deuterium abundance, the maximum allowable baryonic contribution decreases to $\Omega_b h_{50}^2 \leq 0.04$ ($\eta \leq 2.6 \times 10^{-10}$) for spherical shell geometry, or $\Omega_b h_{50}^2 \leq 0.03$ ($\eta \leq 2.1 \times 10^{-10}$) for condensed spheres. A high primordial lithium abundance would increase both of these limits to $\Omega_b h_{50}^2 \leq 0.06$.

Figures 3-3, 3-4, 3-5, and 3-7 show contours of allowed parameters in the r versus η and r versus $\Omega_b h_{50}^2$ plane for the adopted light-element abundance constraints of Eqs. (III-2) - (III-4) and for a possible Lyman-α D/H of Eqs. (III-11) and (III-12), for the condensed sphere, spherical shell, condensed cylinder, and cylindrical shell fluctuation

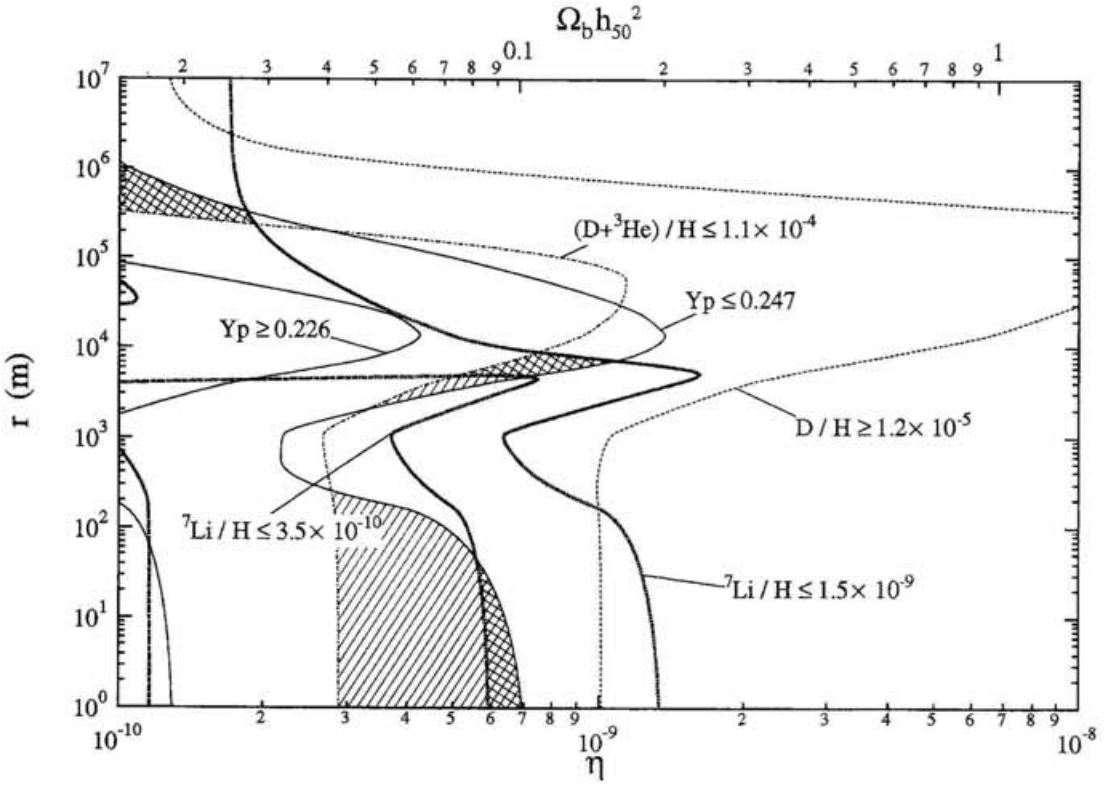

Figure 3-1: Contours of allowed values for baryon-to-photon ratio η (or $\Omega_b h_{50}^2$) and fluctuation separation radius r based upon the various light-element abundance constraints as indicated. The separation r is given in units of meters comoving at $kT = 1$ MeV. This calculation is based upon baryon density fluctuations represented by condensed spheres. The double cross hatched region corresponds to the allowed region based upon the adopted primordial abundance limits (Copi et al. 1995b). The single cross hatched region depicts the allowed parameters if an extreme ^{7}Li upper limit is allowed.

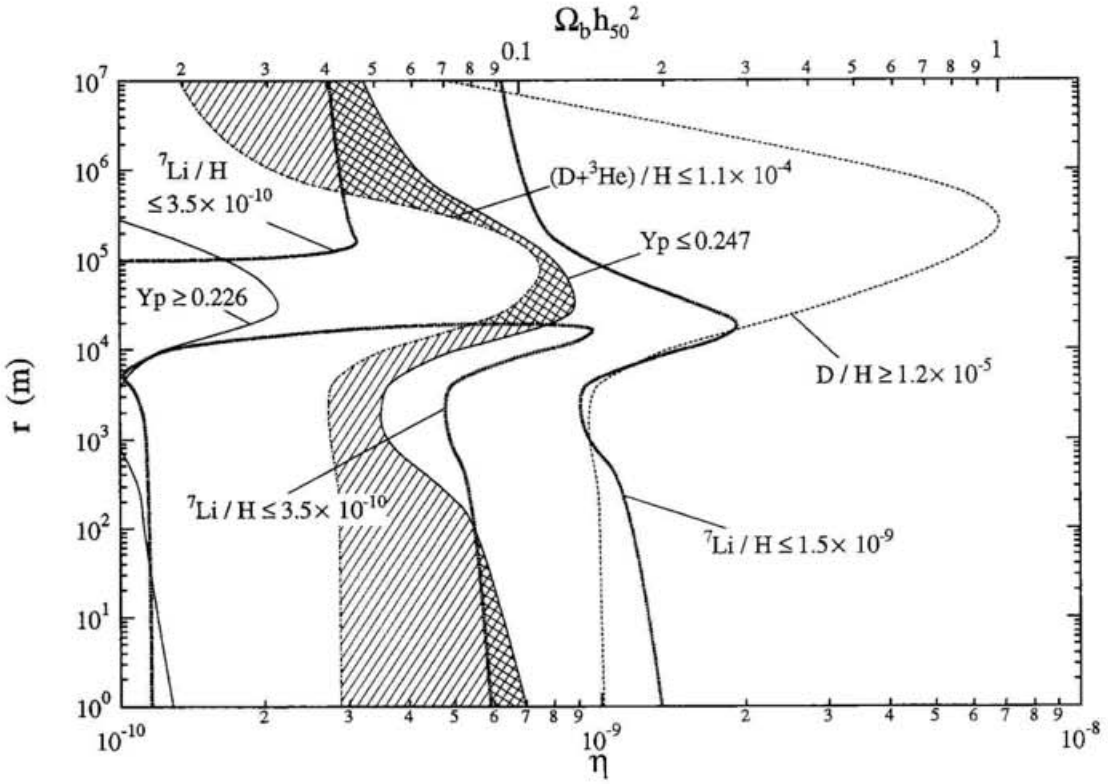

Figure 3-2: Same as Figure 3-1, but for fluctuations represented by spherical shells.

geometries, respectively. The fluctuation cell radius r is given in units of meters for a comoving length scale fixed at a temperature of $kT = 1\,\mathrm{MeV}$. Both of the possible ^{7}Li limits, Eqs. (III-3) and (III-4) which we have discussed above, are also drawn as indicated. In order to clearly distinguish the two abundance constraints, we use the single and double-cross hatches for the regions allowed by the adopted lower (Eq. (III-3)) and higher (Eq. (III-4)) limits to the ^{7}Li primordial abundance.

Even in the IBBN scenario, if the low D/H of Eq. (III-12) (Burles & Tytler 1996) is adopted as primordial, this range for D/H appears to be compatible with the ^{7}Li abundance only when a higher (Population I) primordial ^{7}Li abundance limit is adopted, except for a very narrow region of $\eta \sim 6\times10^{-10}$ and $r \leq 10^2\,m$. This conclusion remains unchanged for any other fluctuation geometries. Therefore, the acceptance of the low (Burles & Tytler 1996) value of D/H would strongly suggest that significant depletion of ^{7}Li has occurred.

In contrast, adoption of the high D/H of Eq. (III-11) (Rugers & Hogan 1996a) as primordial allows the concordance of all light-elements. The upper limits to η and $\Omega_b\, h_{50}^2$ are largely determined by D and ^{7}Li. The concordance range for the baryon density is comparable to that for HBBN for small separation distance r. However, there exist other regions of the parameter space with optimum separation distance, which roughly corresponds to the neutron diffusion length during nucleosynthesis (Mathews et al. 1990), with an increased maximum allowable value of the baryonic contribution to the closure density to $\Omega_b\, h_{50}^2 \leq 0.05$ for the cylindrical geometry, as displayed in Fig. 3-7. This is similar to the value for spherical shells as shown in Mathews et al. (1996) and also in Fig. 3-4 in the present work. The condensed sphere limits, however, are essentially unchanged from those of the HBBN model. If the primordial ^{7}Li abundance could be as high as the upper limit of Li/H $\leq 1.5 \times 10^{-9}$, the maximum allowable

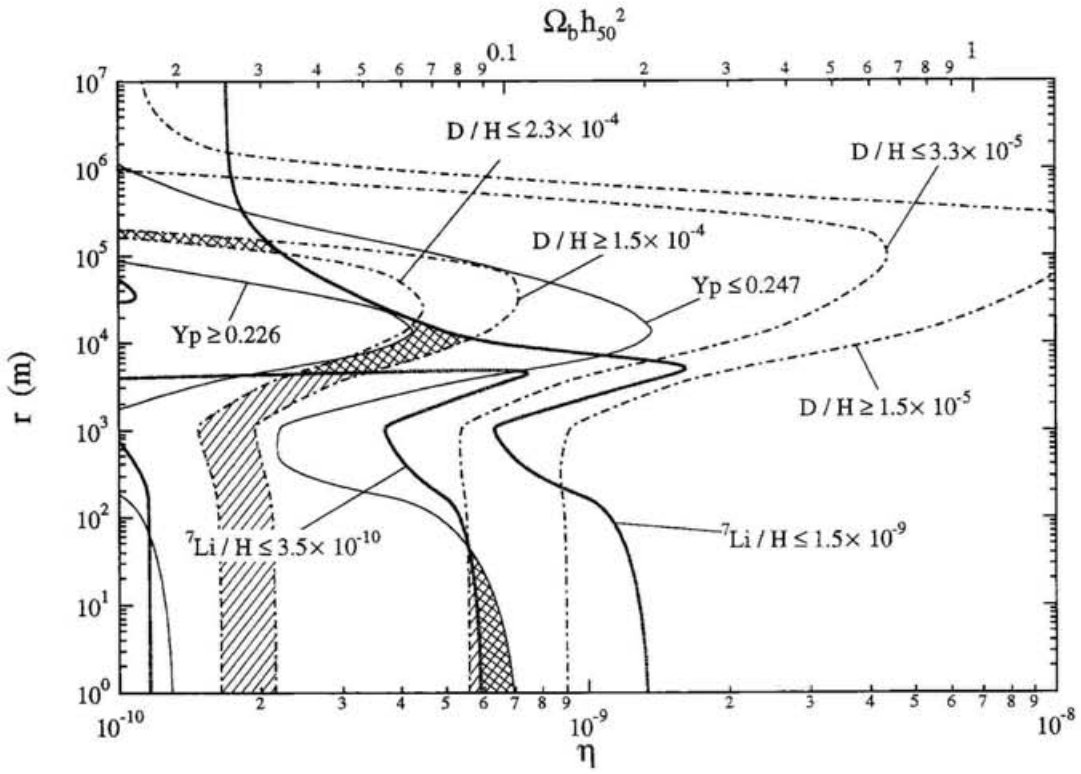

Figure 3-3: Contours of allowed values for baryon-to-photon ratio η (or $\Omega_b h_{50}^2$) and fluctuation separation radius r based upon the various light-element abundance constraints as indicated. The separation r is given in units of meters comoving at $kT = 1\,\mathrm{MeV}$. This calculation is based upon baryon density fluctuations represented by condensed spheres. The cross hatched region is allowed by the adopted primordial abundance limits with high (Eq. (III-11)) and low (Eq. (III-12)) deuterium abundance in Lyman limit systems and also a higher extreme ^{7}Li upper limit (Eq. (III-4)). The single hatched region depicts the allowed parameters for lower ^{7}Li (Eq. (III-3)) constraint. Note that the ^{7}Li abundance is the sum of ^{7}Li and ^{7}Be.

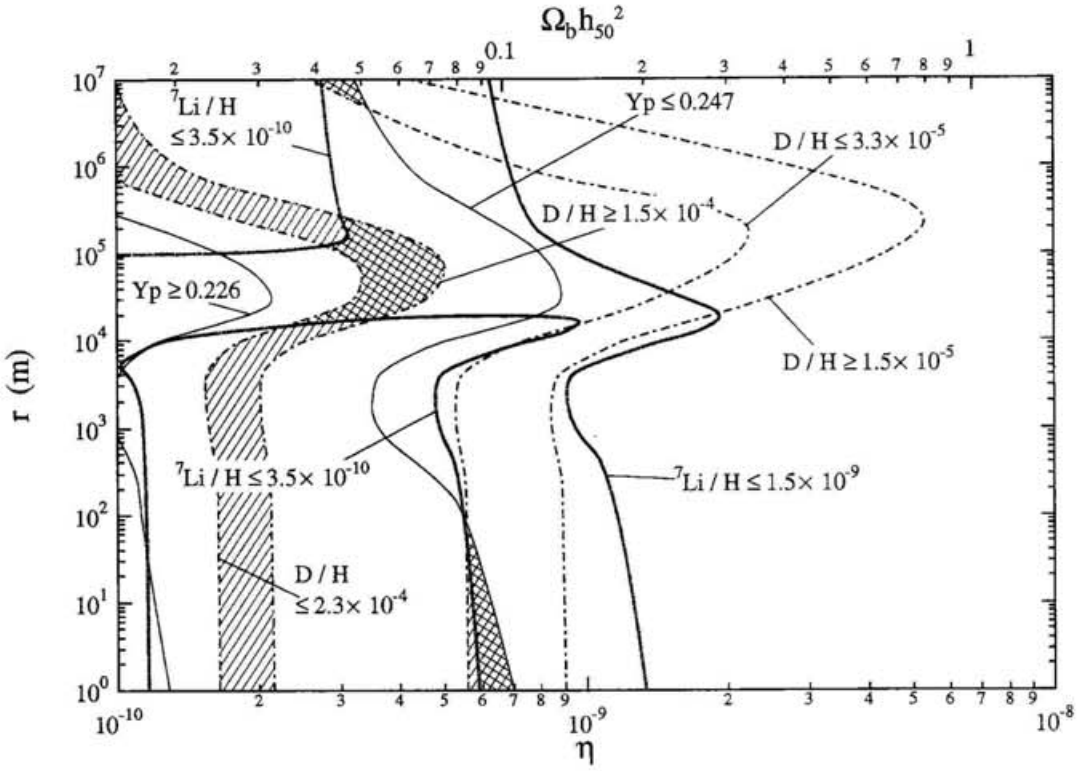

Figure 3-4: Same as Fig. 3-3, but for fluctuations represented by spherical shells.

value of the baryonic content for the condensed sphere would increase to $\Omega_b\, h_{50}^2 \leq 0.08$, with similar values for the spherical shell (Mathews, Kajino & Orito 1996). For both the condensed cylinders and cylindrical shells, the upper limits could be as high as $\Omega_b\, h_{50}^2 \leq 0.1$ as shown in Figs. 3-5 and 3-7. These higher upper limits relative to those of the HBBN are of interest since they are consistent with the inferred baryonic mass in the form of hot X-ray gas (White et al. 1993; White and Fabian 1995) in dense galactic clusters. The acceptance of this consistency, as noted above, requires the significant stellar depletion of ^{7}Li.

In Figures 3-6 and 3-8, we also show contours for the condensed cylinder and cylindrical shell geometries, respectively, but this time with the conventional light-element constraints of Eqs. (III-2), (III-3), (III-5), and (III-10) as indicated. Since the results for the condensed sphere and spherical shell geometries with this set of the conventional

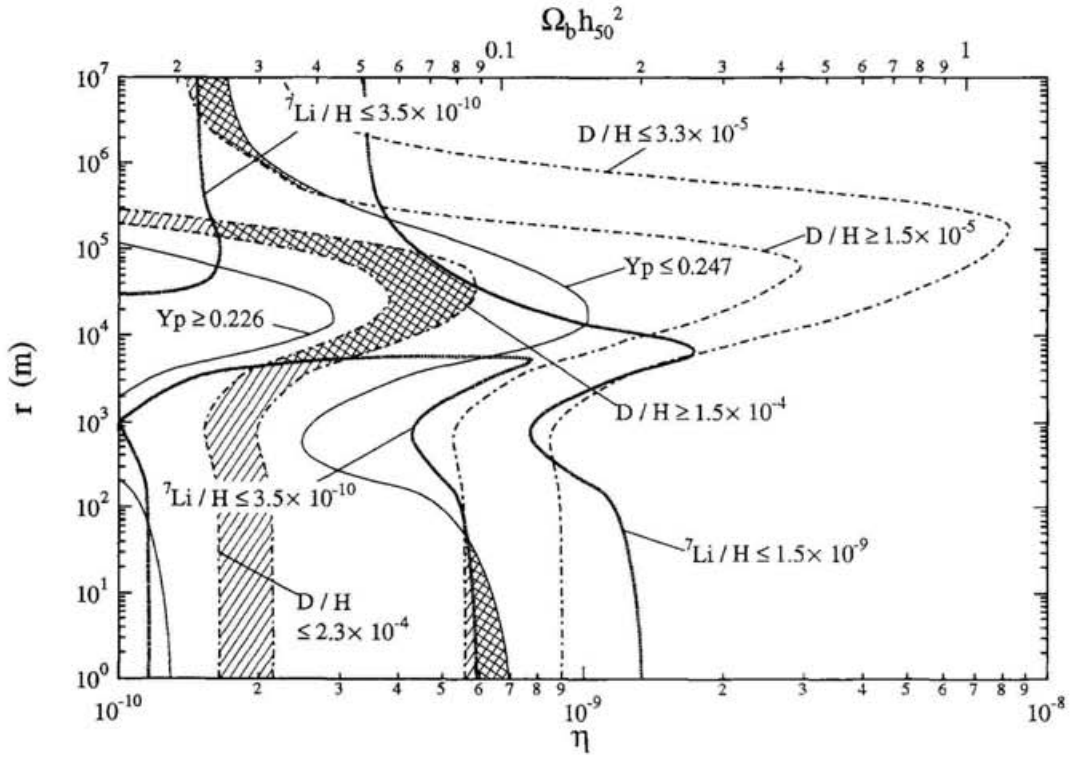

Figure 3-5: Same as Fig. 3-3, but for fluctuations represented by condensed cylinders. Adopted primordial deuterium abundance constraints are inferred from observations of Lyman limit systems (Eqs. (III-11) and (III-12)).

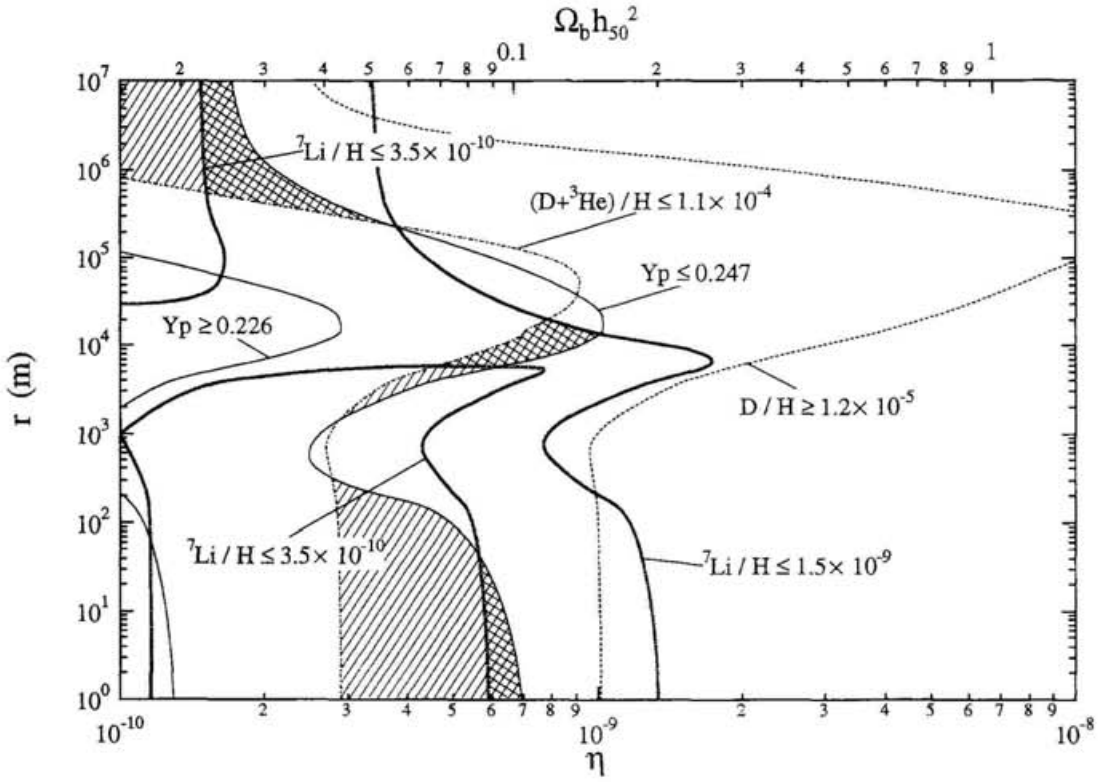

Figure 3-6: Same as Fig. 3-3, but for fluctuations represented by condensed cylinders. Adopted primordial deuterium and ^{3}He abundance constraints are inferred from observations of ISM (Eqs. (III-5) and (III-10)).

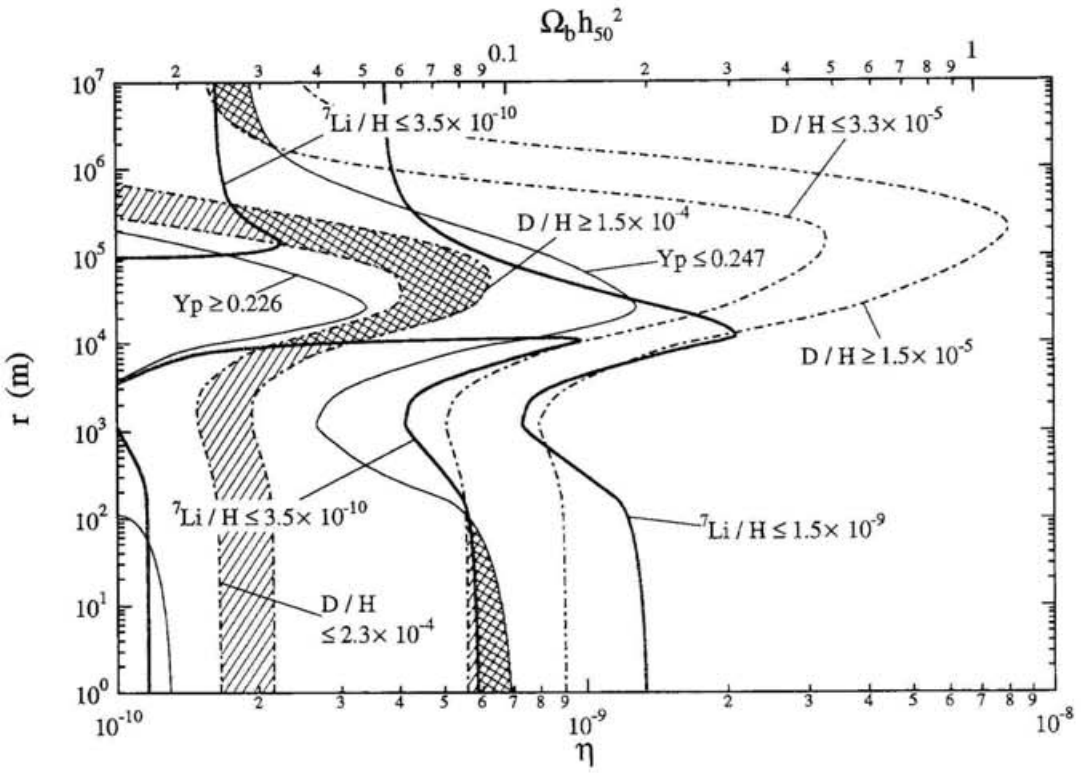

Figure 3-7: Same as Fig. 3-6, but for fluctuations represented by cylindrical shells.

abundance constraints have already been discussed by Mathews et al. (1996), we do not show those contours here. The cylindrical shell geometry of the present work gives the highest allowed value of $\Omega_b h_{50}^2$. Figure 3-8 shows that the upper limits to η and $\Omega_b h_{50}^2$ are largely determined by Y_p and ^{7}Li. The upper limits for a cylindrical shell geometry could be as high as $\Omega_b h_{50}^2 \leq 0.13$ with similar results for the spherical shell geometry (Mathews, Kajino & Orito 1996). A high primordial lithium abundance would increase the allowable baryonic content to as high as $\Omega_b h_{50}^2 \leq 0.2$. The reason that shell geometries allow for higher baryon densities we attribute to more efficient neutron diffusion which occurs when the surface area to volume area is increased. This allows for more initial diffusion to produce deuterium, and more efficient back diffusion to avoid over producing ^{7}Li.

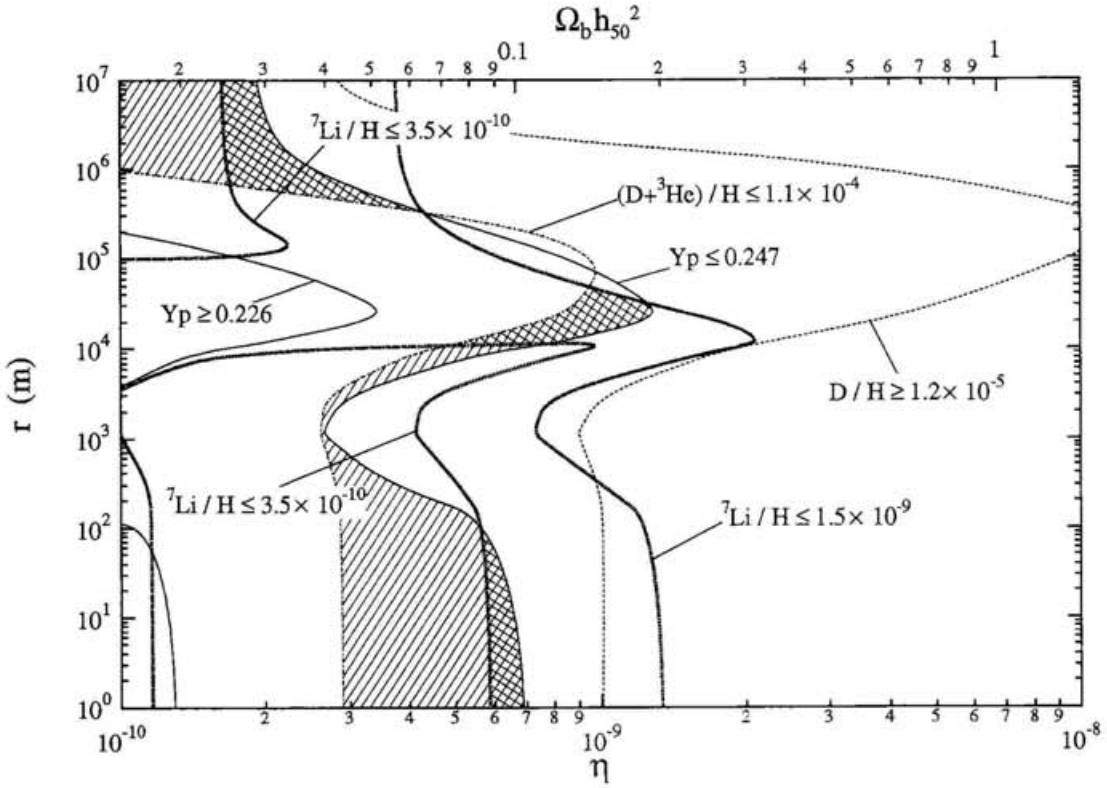

Figure 3-8: Same as Fig. 3-6, but for fluctuations represented by cylindrical shells.

§4 Observational Signature of Baryon Density Inhomogeneities

The production of beryllium and boron as well as lithium in IBBN models can be sensitive to neutron diffusion. Therefore, their predicted abundances are sensitive to not only the fluctuation parameter r, R, and f_v but also the fluctuation geometry (Boyd & Kajino 1989; Malaney & Fowler 1989; Kajino & Boyd 1990; Terasawa & Sato 1990). Figures 4-1 - 4-3 show the contours of the calculated abundances for lithium, beryllium and boron, respectively in the r versus η (and r versus $\Omega_b\ h_{50}^2$) plane. the shaded region depict is allowed values of r and η from the light element abundance constraints [cf. Fig. 3-8] for a cylindrical shell fluctuation geometry. The contour patterns of lithium (Fig. 4-1) and boron (Fig. 4-3) abundances are very similar, whereas there is no similarity found between lithium (Fig. 4-1) and beryllium (Fig. 4-2) abundances.

In order to understand the similarities and differences among these three elemental abundances, we show in Figs. 4-4 and 4-5 the decompositions of the A = 7 abundance into ^{7}Li and ^{7}Be and the boron abundance into ^{10}B and ^{11}B. These Figures show also the dependence of the predicted LiBeB abundances in IBBN on the scale of fluctuations for a cylindrical shell geometry with fixed $\Omega_b\, h_{50}^2 = 0.1$. This value of $\Omega_b\, h_{50}^2$ corresponds to a typical value in the allowable range of η in Fig. 3-8, which optimizes the light element abundance constraints, even satisfying the lower ^{7}Li abundance limit of Eq. (III-3). The fluctuation parameters f_v and R are the same as in Fig. 3-8. Once the baryonic content Ω_b is fixed, the only variable parameter is the separation distance, r.

As can be seen in Fig. 4-4, as the separation r increases, neutron diffusion plays an increasingly important role in the production of t and, by the $^4\mathrm{He}(t,\gamma)^7\mathrm{Li}$ reaction. It works maximally around $r \sim 10^4$ m, which is the typical length scale of neutron diffusion at $kT = 1\,\mathrm{MeV}$. A similar behavior is observed in the $^7\mathrm{Li}(t,n)^9\mathrm{Be}$ reaction.

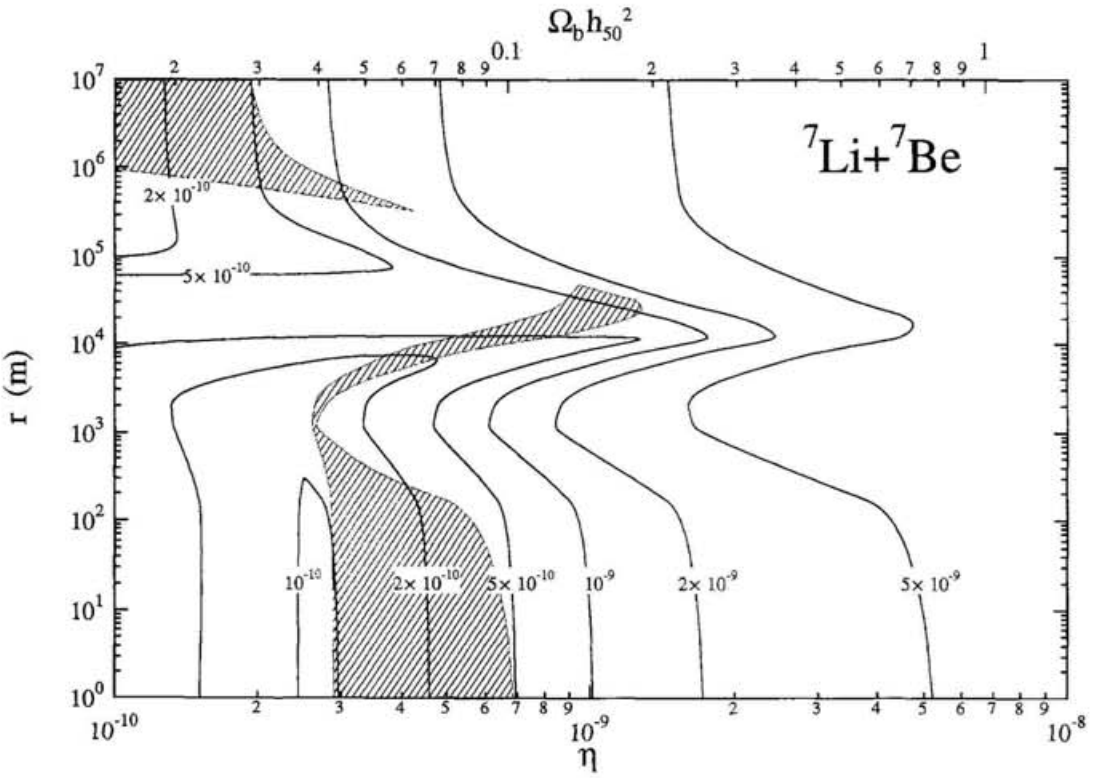

Figure 4-1: Contours of the predicted abundance of lithium (the sum of ^{7}Li and ^{7}Be), for baryon-to-photon ratio η (or $\Omega_b h_{50}^2$) and fluctuation separation radius r, in the cylindrical shell fluctuation geometry. The shaded region displays the allowed $\eta - r$ region from Fig. 3-8.

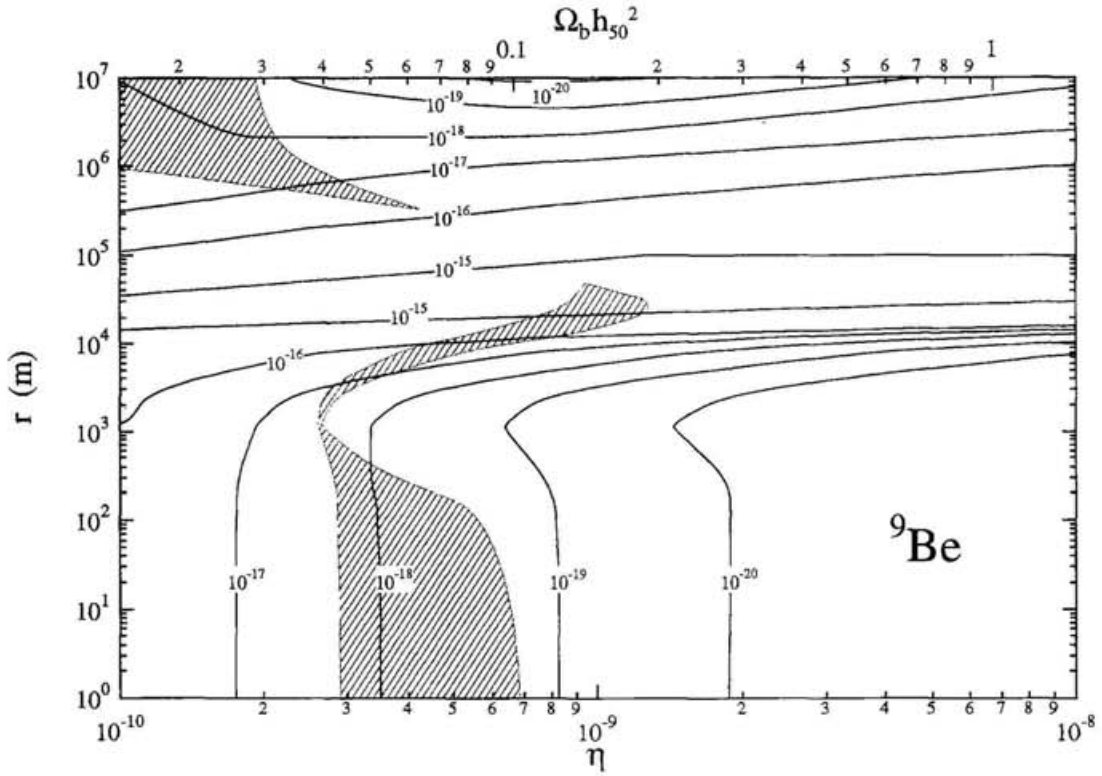

Figure 4-2: Same as Fig. 4-1, but for beryllium, ^{9}Be.

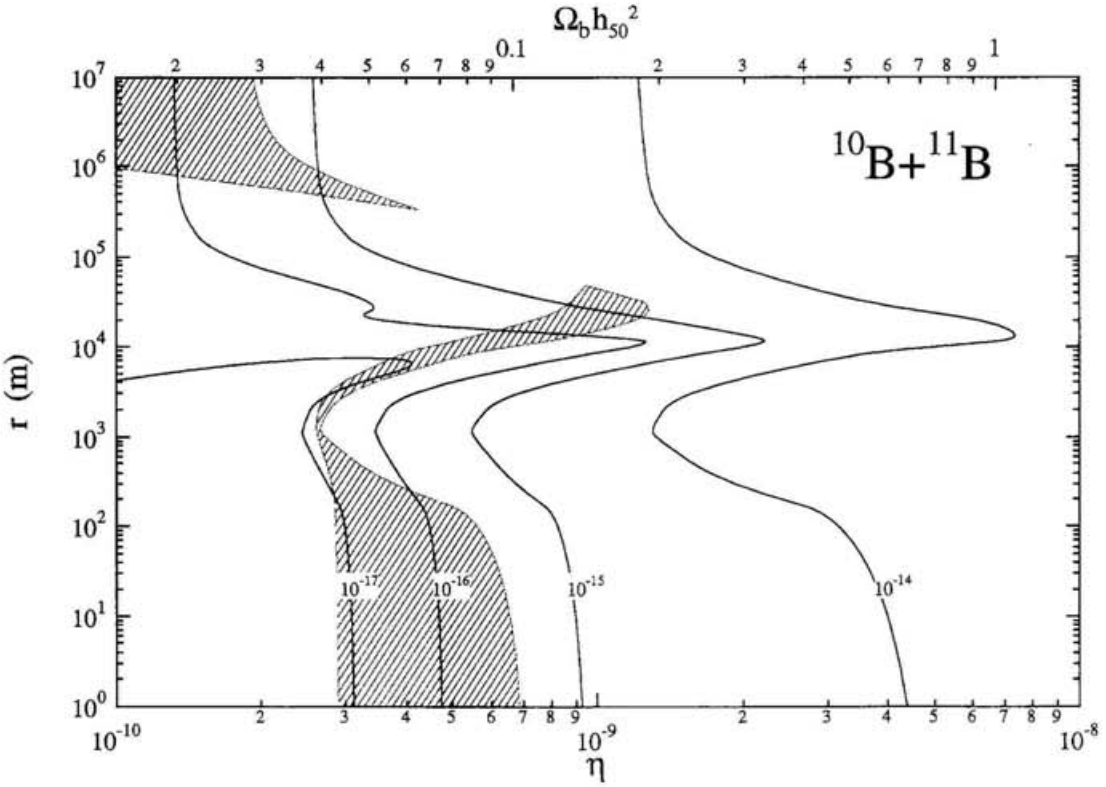

Figure 4-3: Same as Fig. 4-1, but for boron, ^{10}B + ^{11}B.

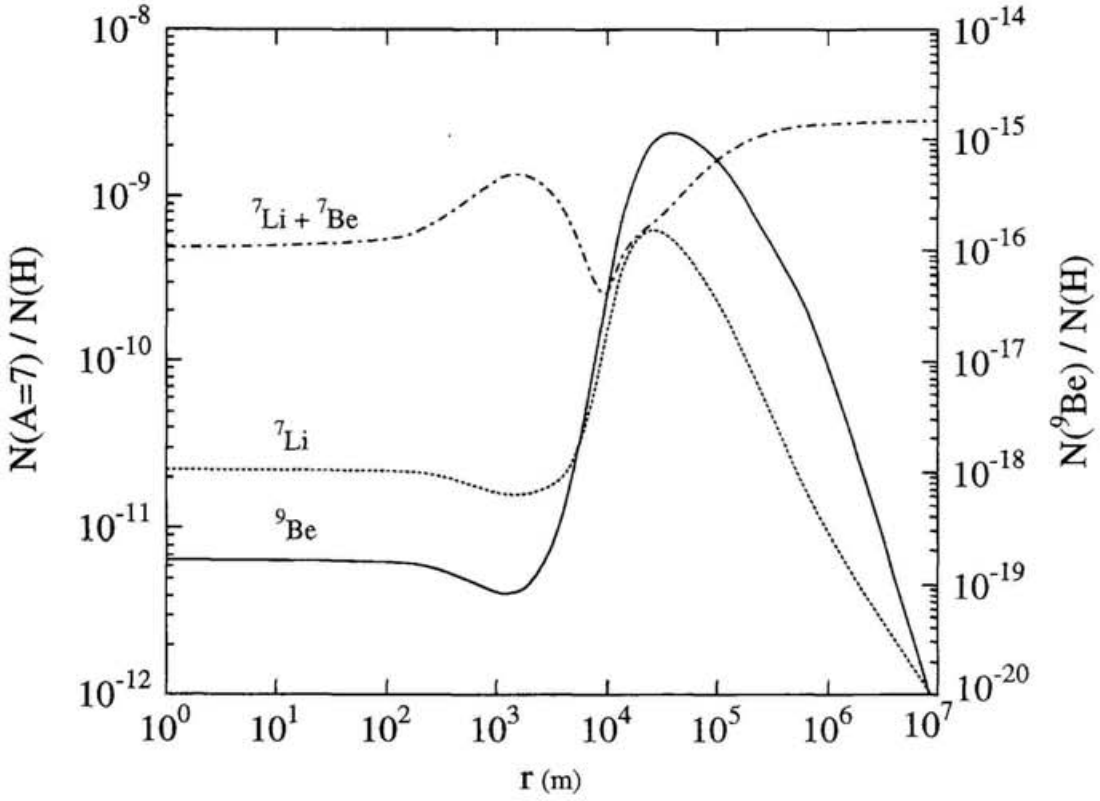

Figure 4-4: Lithium and beryllium abundances as function of proper separation distance in units of meters comoving at $kT = 1\,\mathrm{MeV}$ for fixed $\Omega_b h_{50}^2 = 0.1$. Refer to the abundance scales in *l.h.s.* for lithium and *r.h.s.* for beryllium.

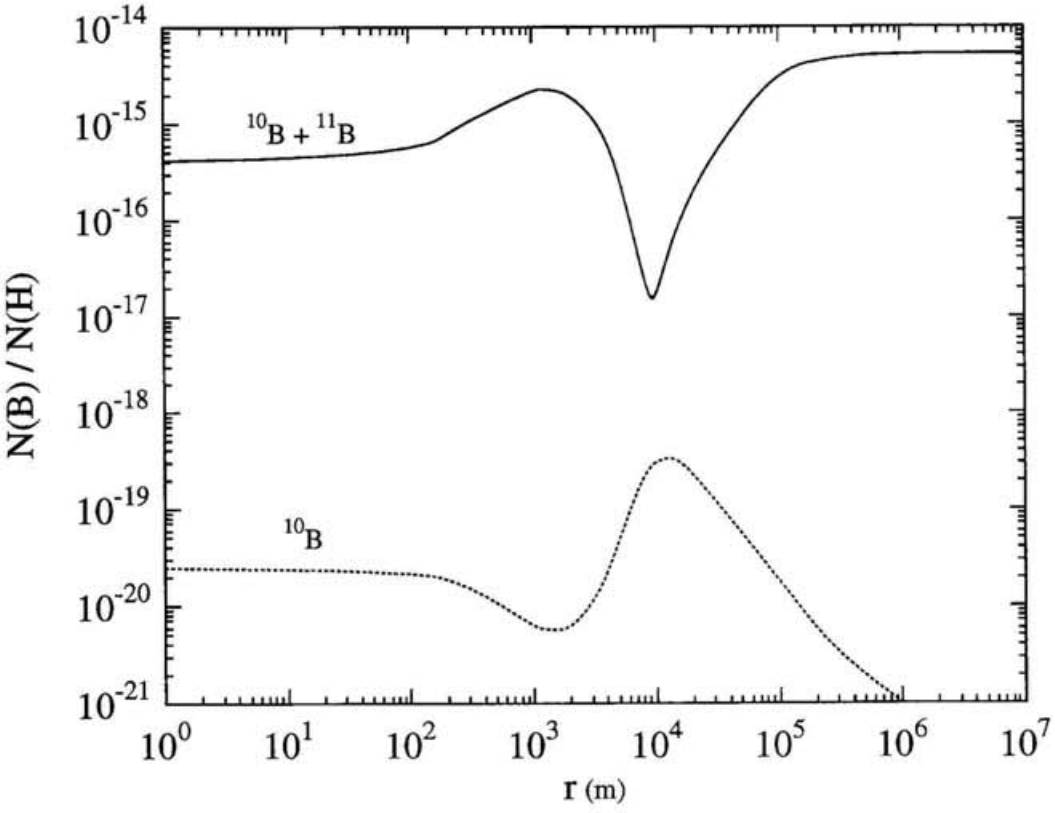

Figure 4-5: Same as Fig. 4-4, but for boron.

This reaction produces most of the ^{9}Be in neutron rich environments where t and ^{7}Li are abundant, as was first pointed out by Boyd and Kajino (1989). At other separation distances r in a $\Omega_b h_{50}^2 = 0.1$ model, most of the A = 7 nuclides are created as ^{7}Be by the ^{4}He(^{3}He, γ)^{7}Be reaction. In the limit of r = horizon scale, the nucleosynthesis products are approximately equal to the sum of those produced in the proton-rich and neutron-rich zones separately (Jedamzik, Fuller, Mathews & Kajino 1994). The predominant contribution from the proton-rich zones makes the ^{7}Be abundance almost constant at larger r, while both ^{7}Li and ^{9}Be decrease as r increases toward the horizon at any separation distance.

Figure 4-5 shows that ^{11}B is a predominant component of the total boron abundance at any separation distance. This is true for almost all values $\Omega_b h_{50}^2$. It has been pointed out (Malaney & Fowler 1988; Applegate, Hogan & Scherrer 1988; Kajino & Boyd 1990) that most ^{11}B is produced by the ^{7}Li$(n,\gamma)^8$Li$(\alpha,n)^{11}$B reaction sequence in neutron-rich environments at relatively early times when most of the other heavier nuclides are made. Recent measurements of the previously unmeasured ^{7}Li(α,n)^{11}B reaction cross section (Boyd et al. 1992; Gu et al. 1995; Boyd, Paradellis & Rolfs 1996) at the energies of cosmological interest have removed the significant ambiguity in the calculated ^{11}B abundance due to this reaction. The factor of two discrepancy among several different measurements of the reaction cross section for ^{7}Li$(n,\gamma)^8$Li was also resolved by the new measurement (Nagai et al. 1991). The ^{7}Li$(\alpha,\gamma)^{11}$B reaction also makes an appreciable but weaker contribution to the production of ^{11}B in the neutron-rich environment. In the proton-rich environment, on the other hand, the ^{7}Be$(\alpha,\gamma)^{11}$C reaction contributes largely to the production of ^{11}C which beta decays to ^{11}B in 20.39 min. These facts explain why the contour patterns of the lithium and boron abundances in Figs. 4-1 and 4-3 look very similar.

It is conventional in the literature to quote the beryllium and boron abundance relative to H = 10^2. Hence, one defines the quantity [X] = 12+log(X/H). In cylindrical shell fluctuation geometry the beryllium abundance can take the value of [Be] ~ -3 while still satisfying all of the light-element abundance constraints and the Population II lithium abundance constraint (Figs. 4-1 and 4-2). This abundance is higher by three orders magnitude than that produced in the HBBN model with conventional light-element abundance constraints. This result is contrary to a recent result with the condensed sphere geometry and for a more restricted parameter space (Thomas et al. 1994). Recent beryllium observation of Population II stars (Rebolo et al. 1988; Ryan et al. 1990, 1992; Ryan 1996; Gilmore et al. 1992a,1992b; Boesgaard & King 1993; Boesgaard 1994, 1996a,b) have placed the upper limit on the primordial ^{9}Be abundance to [Be] ~ -2, one order magnitude greater than the beryllium abundance in the IBBN cylindrical model.

The calculated boron abundance at the optimum separation distance is essentially equal to the value of the HBBN model. However, a high primordial lithium abundance would increase the upper limit to $\Omega_b h_{50}^2$. In this case, the boron abundance could be one or two orders magnitude larger than that of the HBBN model (Fig. 4-3).

It has been a standard interpretation Yoshii, Mathews, & Kajino 1995 that Be and B were produced by the spallation process of cosmic-ray protons and alpha-particles interacting with interstellar CNO medium. Since the production in this mechanism is secondary after the creation of seed CNO elements, it is impossible to find Be and B in metal-weak halo dwarfs where the CNO abundances were not enough when the first generation stars were born about 10^{10} years ago. However, amounts of Be have been detected in many population II dwarfs. Their abundance level is at least two orders of magnitude larger than the HBBN but in reasonable agreement with the IBBN predic-

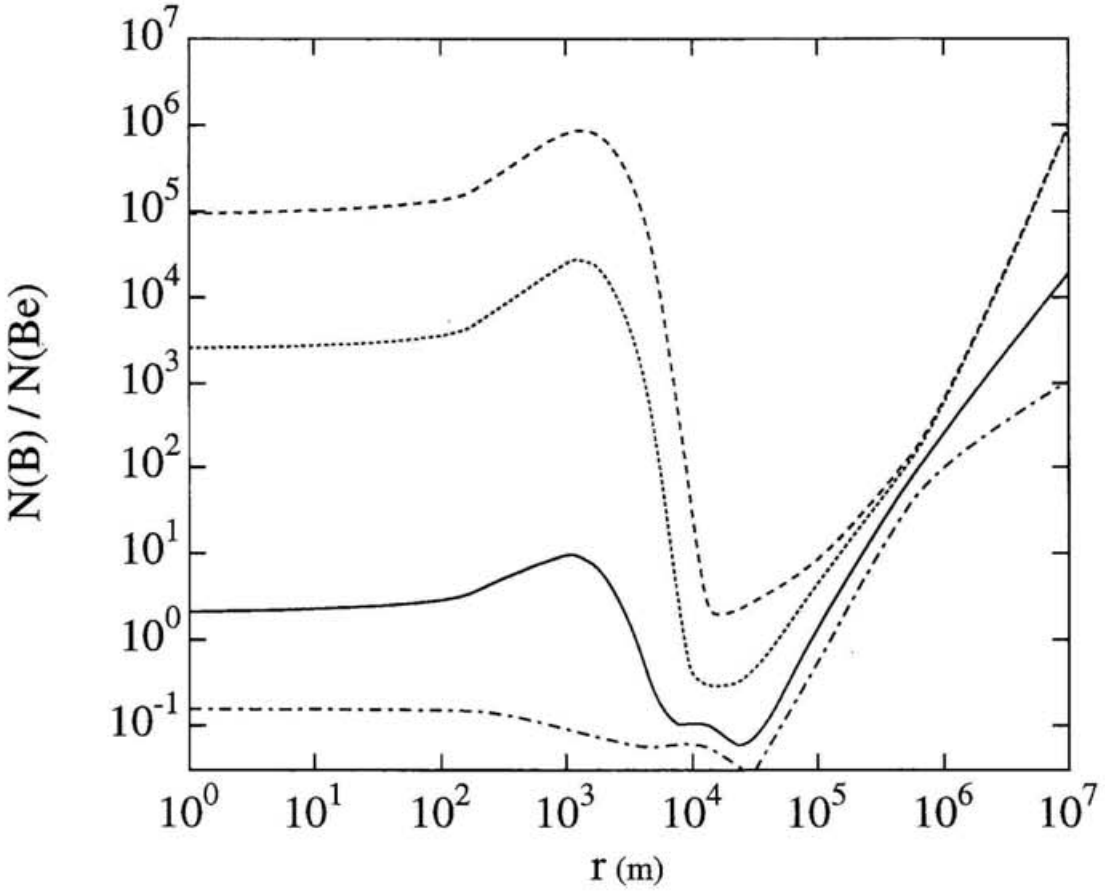

Figure 4-6: Lithium and beryllium abundances as function of proper separation distance in units of meters comoving at $kT = 1\,\mathrm{MeV}$. The dashed, dotted, solid and dash dotted curve correspond to fixed $\Omega_b\, h_{50}^2$ of 0.2, 0.1, 0.04 and 0.024, respctivily.

tion (Kajino & Boyd 1990). Note that the cross section of Be and B production through spallation process is essentially independent on the incident cosmic-ray particle energy, because the largest contribution to the Be and B abundance comes from interaction of high energy protons with CNO nuclides and these cross section are independent of the energy of the incident proton at high energy range Kajino & Boyd 1990. Therefore the ratio of Be and B abundance which were produced by spallation process is determined by the ratio of cross section of each nuclide production induced by high energy cosmic-ray protons. Recent observation has been suggested that the value of B/Be ratio is 10 (Boesgaard 1996a). This results are consistent with the formation of B and Be by cosmic ray spallation of C, N, O nuclei onto protons. In HBBN theory, predicted B and Be ratio is 10^3 with $\Omega_b h_{50}^2 = 0.1$ and is inconsistent with observation. However, IBBN model predicts that while satisfying light elemet abundance constraints, the ratio of B and Be abundance is $\sim 10 - 100$ as can be seen in Figure 4-6.

The heavy element abundances are also considerably enhanced in IBBN (Kajino, Mathews & Fuller 1990; Jedamzik, Fuller & Mathews 1994) from those in HBBN with same baryon density, as can be seen in Fig. 4-7.

Recently, high red-shift ($z \approx 2$) QSO's were found (Pettini & Hunstead 1990) to show strong absorption lines from heavy atomic nuclides C, O, Si, S, Fe, etc. Their observed abundances are ($\approx 1/1000$) relative to the solar and consistent with the detection in most metal deficient star (Bessell & Norris 1984). High red-shift QSO's are believed to be progenitors of present-day disk galaxies at a time when they were still undergoing gravitational collapse and most of their mass resided in the interstellar medium. These heavy elements may suggest some cosmological origin. More detection of the heavy element abundances in old metal-weak dwarfs in the halo and unprocessed intergalactic medium is highly desirable.

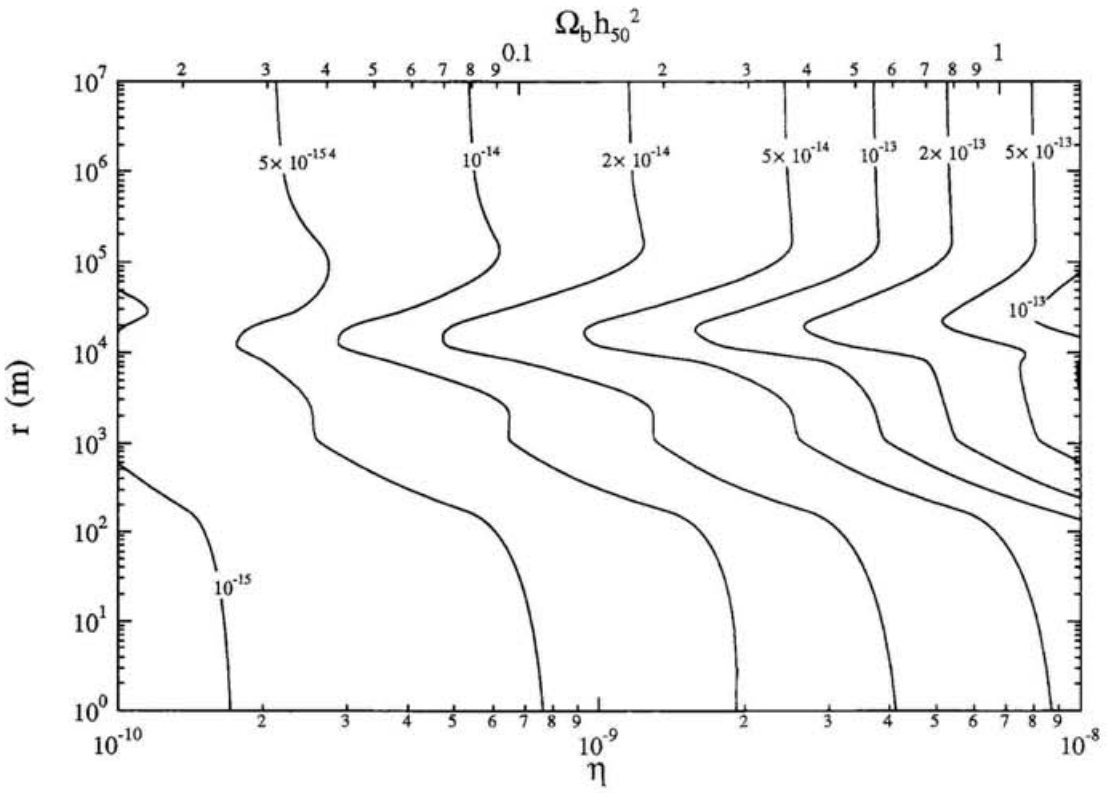

Figure 4-7: Contours of the predicted abundance of the sum of the nuclides which have mass greater than 12, for baryon-to-photon ratio η (or $\Omega_b h_{50}^2$) and fluctuation separation radius r, in the cylindrical shell fluctuation geometry.

§5 Conclusion and Summary

We discussed in this thesis that the non-equilibrium baryon transfer process associated with the first order cosmological QCD phase transition can create a strongly inhomogeneous baryon-density distribution. This makes a dramatic impact on cosmological problems: First, the universal baryonic mass can be as large as $\Omega_B \leq 0.13$ in the inhomogeneous big-bang model for primordial nucleosynthesis, which is in reasonable agreement with recent astronomical observation. Second, with this result on Ω_b, it becomes more likely that some appreciable part of dark matter for $\Omega_{DYN} \approx 0.1 - 0.3$ may possibly originate from baryons.

In view of this, there is now stronger motivation than ever to study the quark-hadron phase transition, based on deep understandings of the rich and profound nature of QCD.

We have investigated the upper limit to η and $\Omega_b\, h_{50}^2$ in inhomogeneous primordial nucleosynthesis models. We have considered effects of various geometries. In particular, for the first time we consider cylindrical geometry. We have also incorporated recently revised light-element abundance constraints including implications of the possible detection (Songaila et al. 1994; Carswell et al. 1994; 1996; Tytler & Fan 1994; Tytler, Fan, & Burlers 1996; Rugers & Hogan 1996a, 1996b; Wampler et al. 1996) of a high deuterium abundance in Lyman-α absorption systems. We have shown that with low primordial deuterium (Tytler & Fan 1994; Tytler, Fan, & Burlers 1996), significant depletion of ^{7}Li is required to obtain concordance between predicted light-element abundance of any model of BBN and the observationally inferred primordial abundance. If high primordial deuterium (Rugers & Hogan 1996a) is adopted (Eq. (III-11)), there is a concordance range which is largely determined by D/H, and the upper limit to $\Omega_b\, h_{50}^2$ is 0.05. However, with the presently adopted (Eqs. (III-2), (III-4), (III-5), (III-10))

light-element abundance constraints (Schramm & Mathews 1995; Copi, Schramm & Turner 1995; Olive & Scully 1996), values of $\Omega_b\, h_{50}^2$ as large as 0.2 are possible in IBBN models with cylindrical-shell fluctuation geometry.

We have also found that significant beryllium and boron production is possible in IBBN models without violating the light element abundance constraints. The search for the primordial abundance of these elements in low metallicity stars could, therefore, be a definitive indicator of the presence or absence of cylindrical baryon inhomogeneities in the early universe.

REFERENCES

Aarnio, P. et al. (DELPHI Collaboration) 1989, Phys. Lett. B., 231, 539

Abrams, G. S. et al. 1989, Phys. Rev. Lett., 63, 724

Adeva, B. et al. (L3 Collaboration) 1992, Phys. Lett. B., 275, 209

Alcock, C. R., Dearborn, D. S., Fuller, G. M., Mathews, G. J., & Meyer, B. S. 1990, Phys. Rev. Lett., 64, 2607

Alcock, C. R., Fuller, G. M., & Mathews, G. J. 1987, ApJ, 320, 439

Alcock, C. et al. 1993, Nature, 365, 621

ALEPH collaboration. 1990, Phys. Lett. B., 235, 399

Andersson, B., Gustafson, G. & Sjostrand, T. 1982, Nucl. Phys. B., 197, 45

Applegate, J. H. & Hogan, C. J. 1985, Phys. Rev. D., 30, 3037.

Applegate, J. H., Hogan, C. J., & Scherrer, R. J. 1987, Phys. Rev. D., 35, 1151

Applegate, J. H., Hogan, C. J., & Scherrer, R. J. 1988, ApJ, 329, 592

Ashman, K. M. 1992, PASP, 104, 1109

Aubourg, E. et al. 1993, Nature, 365, 623

Balbes, M. J., et al. 1993, ApJ, 418, 229

D.S. Balser, D. S. et al. 1994, ApJ, 430, 667

de Bernardis, P., et al. 1994, ApJ, 422, L33

de Bernardis, P., de Gasperis, G., Masi, S. & Vittorio, N. 1994, ApJ, 433, L1

Bessell, M.S. & Norris, J. 1984, ApJ, 285, 622

Boesgaard, A. M., & King, J. R. 1993 AJ 106, 2309

Boesgaard, A. M. 1994, in *Proceeding of the ESO Workshop on the Light Elements*, Crane, P., eds

Boesgaard, A. M. preprint, 1996a, to appear in Astronomical Society of the Pacific Conference Proceedings on *Formation of the Galactic Halo-Inside and Out*, Morrison, H. & Sarajedini, A., eds

Boesgaard, A. M. 1996b, private communication.

Boyd, R. N. & Kajino, T. 1989, ApJ, 336, L55

Boyd, R. N. et al. 1992, Phys. Rev. Lett., 68, 1283

Boyd, R. N., Paradellis, T. & Rolfs, C. 1996, Comments in Nucl. Part. Physics 22, 47

Brown, L. E. & Schramm, D. N. 1988, ApJ, 329, L103

Brower, R., Huang, S., Potvin, J., & Rebbi, C. 1992, Phys. Rev. D., 46, 2703

Burles, S. & Tytler, D. 1996, ApJ, 460, 584; preprint., astro-ph/9603070, submitted to Science

Carswell, R. F. et al. 1994, MNRAS, 428, 574

Carswell, R. F. et al. 1996, MNRAS, 278, 506

Charbonnel, C. 1996, ApJ, 453, L41

Casher, A., Neuberger, H. & Nussinov, S. 1979, Phys. Rev. D., 20, 179

Copi, C. J., Schramm, D. N., & Turner, M. S. 1995, 1995, Science, 267, 192,1995, ApJ, 455, L95

Davis, R. L. et al. 1992, Phys. Rev. Lett., 69, 1856

Dearborn, D. S. P., Schramm, D. N., & Steigman, G. 1986, ApJ, 302, 35

Dearborn, D. S. P., Steigman, D. N. & Tosi, M. 1996, preprint., astro-ph/9601117

Denegri, D., Sadoulet, B. & Spiro, M. 1990, Rev. Mod. Phys., 62, 1

Dolgov, A. & Silk, J. 1993, Phys. Rev. D., 47, 4244

Deliyannis, C. P. Demarque, P., & Kawaler, S. D. 1990, ApJS, 73, 21

Deliyannis, C. P., Pinsonneault, M. H. & Duncan, D. K. 1993, ApJ, 414, 740

Deliyannis, C. P., Boesgaard, A. M., & King, J. M. 1995, ApJ, 452, L13

Epstein, R., Lattimer, J. & Schramm, D. N. 1977, Nature, 263, 198

Edmunds, M. G. 1995, MNRAS, 272, 241

Fields, B. D., Kainulainen, K., Olive, K. A. & Thomas, D. 1996, preprint., astro-ph/9603009

Freese, K. & Adams, F. C. 1990, Phys. Rev. D., 41, 2449

Freeman, K. C. *in 6th Asia Pacific Physics Conf.* (1994).

Fukugita, M. & Hogan, C. 1991, Nature, 354, 17

Fuller, G. M., Mathews, G. J., & Alcock, C. R. 1988, Phys. Rev. D., 37, 1380

Fuller, G. M., Jedamzik, K., Mathews, G, J., & Olinto, O 1994, Phys. Lett. B., 333, 135

Gao, M. 1988, Nucl. Phys. B. Suppl., 9, 368

Geiss, J in *Origin and Evolution of the Elements*, ed. N. Prantzos et al. (Cambridge University Press, 1993) p.89.

Gilmore, G., Edvardsson, B., & Nissen, P. E. 1992a, ApJ, 378, 17

Gilmore, G., Gustafsson, B., Edvardsson, B., & Nissen, P. E. 1992b, Nature, 357, 379

Glendenning, N. K. & Matsui, T. 1983, Phys. Rev. D., 28, 2890

Gloeckler, G. & Geiss, J. 1996, Nature, 381, 210

Gottlieb, S. 1991, Nucl. Phys. B., 20, 247

Gu, X. et al. 1995, Phys. Lett. B., 343, 31

Hata, N., Scherrer, R. J., Steigman, G., Thomas, D. & Walker, T. P. 1995, Phys. Rev. Lett., 75, 3977

Hata, N., Scherrer, R. J., Steigman, G., Thomas, D. & Walker, T. P. 1996, ApJ, 458, 637

Hogan, C. J. 1995, ApJ, 441, L17

Hobbs, L. & Thorburn, J. A. 1994, ApJ, 428, L25

Iwasaki, Y., Kanaya, K., Kaya, S., Sakai, S. & Yoshie, T. 1995, Nucl. Phys. B. Suppl., 42, 499; also, Kanaya, K. (1995) in this volume.

Izatov, Y. I., Thuan, T. X. & Lipovetsky, V. A. 1994, ApJ, 435, 647

Izatov, Y. I., Thuan, T. X. & Lipovetsky, V. A. 1996, submitted to ApJ

Jedamzik, K., Mathews, G., & J.Fuller, G. M. 1995, ApJ, 441, 465

Jedamzik, K., Fuller, G. M., & Mathews, G. J., 1994, ApJ, 423, 50

Jedamzik, K., Fuller, G. M., Mathews, G. J., & Kajino, T., 1994, ApJ, 422, 423

Jedamzik, K., Fuller, G. M., Mathews, G, J., & Olinto, O. 1994b, Phys. Lett. B., 333, 135

Jedamzik, K.& Fuller, G. M. 1994, ApJ, 423, 33

Kajantie, K. and Kurki-Suonio, H. 1986, Phys. Rev. D., 34, 1719

Kajantie, K., Kärkkäinen, L. & Rummukainen, A. 1990, Nucl. Phys. B., 333, 100

Kajantie, K., Kärkkäinen, L. & Rummukainen, A. 1991, Nucl. Phys. B., 357, 693

Kajantie, K., Kärkkäinen, L. & Rummukainen, A. 1992, Phys. Lett. B., 286, 125

Kajino, T. & Boyd, R. N. 1990, ApJ, 359, 267

Kajino, T., Mathews, G. J., & Fuller, G. M. 1990, ApJ, 364, 7

Kajino, T. 1991, Nucl. Phys. B. Suppl., 24, 74

Kajino, T. & Tassie, L. J. 1993, J. J. Appl. Phys., 9, 168

Kajino, T., Orito, M., Suganuma, H. & Yamamoto, T. 1996 in preparation.

Kanaya, K. 1990, Nucl. Phys. B. Suppl., 47, 144

Kawano, L. H., Fowler, W. A., Kavanagh, R. W., & Malaney, R. A., 1991, ApJ, 372, 1

Krauss, L. M. & Romanelli, P. 1990, ApJ, 358, 47

Krauss, L. M. & Peter, J. K., 1994, preprint, astro-ph/9405004

Krauss, L. M. & Kernan, P. J. 1994, ApJ, 432, L79

Kurki-Suonio, H., & Matzner, R. A. 1989, Phys. Rev. D., 39, 1046

Kurki-Suonio, H., & Matzner, R. A. 1990, Phys. Rev. D., 42, 1047

Kurki-Suonio, H., Matzner, R. A., Olive, K. A., & Schramm, D. N. 1990, ApJ, 353, 406

Kurki-Suonio, H., Matzner, R. A., Centrella, J., Rothman, T., & Wilson, J. R. 1988, Phys. Rev. D., 38, 1091

Kurucz, R. L. 1995, ApJ, 452, 102

Landau, L. D. & Lifshitz, E. M. *Statistical Physics* (Pergamon, New York, 1969).

Linsky, J. L., Brown, A., Gayley, K., Deplas, A., Savage, B. D., Ayres, T. R., Landsman, W., Shore, S. W. & Heap, S 1993, ApJ, 402, 694

Linsky, J. L. et al., 1995, ApJ, 451, 335

Malaney, R. A. & Fowler, W. A. 1988, ApJ, 333, 14

Malaney, R. A. & Fowler, W. A. 1989, ApJ, 345, L5

Malaney, R. A. & Butler, M. N. 1989, Phys. Rev. Lett., 62, 117

Malaney, R. A. & Mathews, G. J. 1993, Phys. Rep., 229, 145

Mather, J. C., et al. 1990, ApJ, 354, L37

Mather, J. C., et al. 1994, ApJ, 420, 449

Mathews, G. J., Meyer, B. S., Alcock, C. R., & Fuller, G. M. 1990, ApJ, 358, 36

Mathews, G. J., Boyd, R. N. & Fuller, G. M. 1993, ApJ, 403, 65

Mathews, G. J., Kajino, T. & Orito, M. 1996, ApJ, 456, 98

Mathews, G. J., Schramm, D. N., & Meyer, B. S. 1993, ApJ, 404, 476

McCullough, P. R. 1992, ApJ, 390, 213

Nagai, Y. et al. 1991, ApJ, 381, 444

Nelson, A. 1990, Phys. Lett. B., 240, 179

Orito, M., Kajino, T., Boyd, R. N. & Mathews, G. J. 1995, ApJ, to be submitted

Olive, K. A. & Steigman, G. 1995, ApJS, 97, 49

Olive, K. A., Schramm, D. N., Steigman, G., & Walker, T. 1990, Phys. Lett. B., 238, 454

Olive, K. A. & Scully, S. T. 1996, IJMPA, 11

Particle Data Group, 1994, Phys. Rev. D., 50, 1173

Pagel, B. E. J., Simonson, E. A., Terlevich, R. J. & Edmunds, M. 1992, MNRAS, 255, 325

Pagel, B. E. J. 1993, Phys. Rep., 227, 51

Pasachoff, J. M. & Vidal-Madjar, A. 1989, Comm. Astrophys, 14, 61

Persic, M. & Salucci, P. 1992, MNRAS, 258, 148

Petersson, B. 1993, Nucl. Phys. B. Suppl., S30, 66

Pettini, A. & Hunstead, D. 1990, Aust. J. Phys., 43, 227

Pinsonneault, M. H., Deliyannis, C. P. & Demarque, P. 1992, ApJS, 78, 179

Rauscher, T., Applegate, J. H., Cowan, J. J., Thielemann, F. K., & Wiescher, M. 1994, ApJ, 429, 499

Rebolo, R., Molaro, P., Abia, C., & Beckman, J. E. 1988, A&A, 193, 193

Reeves, H. 1994, Rev. Mod. Phys., 66, 193

Rood, R. T., Bania, T. M. & . Wilson, T. L. 1992, Nature, 355, 618

Rugers, M. & Hogan, C. J. 1996a, ApJ, 459, L1

Rugers, M. & Hogan, C. J. preprint., astro-ph/9603084; 1996b, A.J, 111, 2135

Ryan, S. G., Bessell, M. S., Sutherland, R. S., & Norris, J. E. 1990, ApJ, 348, L57

Ryan, S. G., Norris, J. E., Bessell, M. S., & Deliyannis, C. P. 1992, ApJ, 388, 184

Ryan, S. G., Beers, T. C., Deliyannis, C. P. & Thorburn, J. A. 1996, ApJ, 458, 543

Ryan, S. G. 1996, private communication

Sasselov, D. & Goldwirth, D. 1995, ApJ, 444, L5

Schramm, D. N. & Wagoner, R. V. 1977, Ann. Rev. Nucl. Part. Sci., 27, 37

Schramm, D. N. & Mathews, G. J. 1995, in *Nuclear and Particle Astrophysics in the Next Millennium*, E. Kolb, et al., eds, (World Scientific; Singapore) in press

Skillman, E., et al. 1994, ApJ, 431, 172

Skillman, E. & Kennicutt, R. C. 1995, ApJ, 411, 655

Smoot, G. F. et al 1992, ApJ, 396, L1

Smith, M. S., Kawano, L. H. & Malaney, R. A., 1993, ApJS, 85, 219

Smith, V. V., Lambert, D. L. & Nissen, P. E. 1992, ApJ, 408, 262

Songaila, A., Cowie, L. L., Hogan, C. J., & Rugers, M. 1994, Nature, 368, 599

Spite, J. & Spite, M. 1982, ,, A&A, 115,, 357

Steigman, G., Schramm, D. N. & Gunn, J. E. 1977, Phys. Lett. B., 176, 33

Steigman, G. & Tosi, M. 1995, ApJ, 453, 173

Steigman, G., 1996a, To appear in the Proceedings of the Workshop on *Theoretical and Phenomenological Aspects of Underground Physics*, Suppl. Nucl. Phys. B, (preprint., astro-ph/9602029)

Steigman, G. 1996b, ApJ, 457, 737

Suganuma, H. Kajino, T & Yamamoto, T. 1997 in preparation.

Sumiyoshi, K., Kusaka, K., Kamio, T. & Kajino, T. 1989, Phys. Lett. B., 225, 10

Sumiyoshi, K., Kajino, T., Alcock, C. & Mathews, G. J. 1990, Phys. Rev. D., 42, 3963

Tassie, L. J. & Kajino, T. 1993, in "Vistas in Astronomy", ed. Namiki et al., (Pergamon Press) 523

Terasawa, N., & Sato, K. 1989a, Prog. Theor. Phys., 81, 254.

Terasawa, N., & Sato, K. 1989b, Phys. Rev. D., 39, 2893

Terasawa, N., & Sato, K. 1989c, Prog. Theor. Phys., 81, 1085

Terasawa, N., & Sato, K. 1990, ApJ, 362, L47

Thomas, D. Schramm, D. N., Olive, K. A., & Fields, B. D. 1993, ApJ, 406, 569

Thomas, D. Schramm, D. N., Olive, K. A., Mathews, G. J., Meyer, B. S. & Fields, B. D. 1994, ApJ, 430, 291

Thorburn, J. A. 1994, ApJ, 421, 318

Trimble, V. 1987, Ann. Rev. of Astr., 25, 425

Turner, M. S., Truran, J. W., Schramm, D. N. & Copi, C. 1996. preprint., astro-ph/9602050, submitted to

Thuan, T. X., Izatov, Y. I., & Lipovetsky, V. A. in "*Interplay between massive star formation, the ISM and galaxy evolution*", ed. D. Kunth, B. Guiderdoni, M. Heydari-Malayeri & T. X. Thuan, (Gif-sur-Yvette: Editions Frontieres), 1996

Tytler, D. & Fan, X. M. 1994, BAAS, 26, 1424

Tytler, D., Fan, X. M. & Burles. S. 1996, Nature, 381, 207

Tytler, D., Burles, S. & Kirkman, D. preprint., astro-ph/9612121

Vauclair, S. & Charbonnel, C. 1995, 295,, A&A, 715,

van den Bergh, A. 1989, Astr. Ap. Rev., 1, 111

Vangioni-Flam, E. & Casse, M. 1995, ApJ, 441, 471

Wagoner, R. V., Fowler, W.A., & Hoyle, F. 1967, ApJ, 148, 3

Wagoner, R. V. 1973, ApJ, 179, 343

Walker, T. P., Steigman, G., Schramm, D. N., Olive, K. A., & Kang, H. 1991, ApJ, 376, 51

Wampler, E. J., et al. 1996, ,, A&A, in, press(preprint., astro-ph/9512084)

Wasserburg, G. J., Boothroyd, A. I. & Sackmann, I.-J. 1995, ApJ, 447, L37

White, S. D. M., Navarro, J. F., Evrard, A. E. & Frenk, C. S. 1993, Nature, 366, 429.

White, D. A., Fabian, A. C. 1995, MNRAS, 273, 72

Witten, E. 1984, Phys. Rev. D., 30, 272

Yang, J., Turner, M. S., Steigman, G., Schramm, D. N., & Olive, K. A. 1984, ApJ, 281, 493

Yoshii, Y., Mathews, G. J., & Kajino, T. 1995, ApJ, 447, 184

Zel'dovich, Ya. B. 1975, Sov. Astr. Lett., 1, 5.